THE CRYSTAL STRUCTURE OF NEPHELINE

by

GILBERT ENGLANDER KLEIN

B.S. in Physics, Case School of Applied Science, 1939
M.S. in Physics, Case School of Applied Science, 1942

SUBMITTED IN PARTIAL FULFILLMENT OF THE
REQUIREMENTS FOR THE DEGREE OF
MASTER OF SCIENCE
at the
MASSACHUSETTS INSTITUTE OF TECHNOLOGY
1947

Signature redacted

Signature of Author .....
Crystallography Laboratory
Department of Geology, May 20, 1947

Signature redacted

Certified by: ....
Thesis Supervisor

Signature redacted

.....
Chairman, Dept. Comm. on Graduate Students

THE CRYSTAL STRUCTURE OF NEPHELINE

by

GILBERT ENGLANDER KLEIN

B.S. in Physics, Case School of Applied Science, 1939
M.S. in Physics, Case School of Applied Science, 1942

SUBMITTED IN PARTIAL FULFILLMENT OF THE
REQUIREMENTS FOR THE DEGREE OF
MASTER OF SCIENCE
at the
MASSACHUSETTS INSTITUTE OF TECHNOLOGY
1947

Signature redacted

Signature of Author .....
Crystallography Laboratory
Department of Geology, May 20, 1947

Signature redacted

Certified by: ....
Thesis Supervisor

Signature redacted

.....
Chairman, Dept. Comm. on Graduate Students

THE CRYSTAL STRUCTURE OF NEPHELINE

by

GILBERT ENGLANDER KLEIN

TABLE OF CONTENTS

LIST OF ILLUSTRATIONS

LIST OF TABLES

ACKNOWLEDGMENTS

The writer wishes to acknowledge the support given by the Owens-Illinois Glass Company during the duration of the project. Without this financial backing, the project would never have been possible.

To Professor Martin J. Buerger, who first suggested the problem and who acted as the guiding spirit, especially when the progress seemed to reach its lowest ebb, I wish to express my sincerest thanks for his understanding and interest in the problem at all times.

The aid given by Miss Gabrielle Hamburger, who for a time worked on the project and performed many of the calculations as well as offering many valuable suggestions, helped greatly in the performance of the work. Mrs. Elsa Barney added her efforts to the completion of the work with the preparation of several of the illustrations.

Lastly, I should like to acknowledge the aid given by my wife, Mrs. Ann S. Klein, who helped me at various times with the performance of various tasks during the progress of the work and who acted to lend moral support when it was needed the most.

Chapter I

INTRODUCTION

In spite of the large amount of work which has been done on the silicate minerals, Bragg[1] points out that there are still a number of structures which are assumed to be composed of linked silicon-aluminum-oxygen tetrahedra which have not been thoroughly investigated up to the present time. Nepheline is one of this group of minerals.

Although a fair amount of preliminary work had been done on nepheline, including the determination of the unit cell dimensions and other physical constants, and Schiebold[2] went so far as to suggest that the structure of nepheline is based on the structure of tridymite, the actual determination of the structure still remained a real trial due to the complexity of the problem and the lack of sufficiently powerful and applicable methods of analysis.

With this background in mind it was decided to undertake the problem of determining the arrangement of the atoms in nepheline. The results which would be forthcoming would then give definite information concerning the packing arrangement of sodium and data as

to the silicon-oxygen and aluminum-oxygen distances.

Since it became necessary to work out a new method of attack for the analysis of the structure of nepheline, an attempt was made to keep the method so general as to be applicable to all structures of this type.

Chapter II

PREVIOUS WORK ON NEPHELINE

The mineralogical and morphological properties of nepheline are well known and may be found in all standard textbooks on mineralogy[3].

The earliest reference to work directly concerning nepheline appears in two articles by H. Baumhauer[4,5] appearing in 1882 and 1891. As early as 1892, Andre Duboin[6,7] synthesized potassium-nepheline crystals which crystallized as orthorhombic prisms.

As a result of etch-figure methods, Baumhauer[8](1894) assigned nepheline to the hexagonal-pyrimidal class. Using both dilute hydrofluoric acid and hydrochloric acid as etchants, he obtained undisputable evidence for assigning nepheline to the above class, and the photomicrographs which he presents easily show the only symmetry to be a six-fold hexagonal axis.

Bowen and Elestad[9] report the findings of Dr. J. Morozewicz[10](1897) to the effect that the mineral nepheline has a constant composition whatever the rock in which it is formed, the fixed composition represented by the formula $K_2Al_2Si_3O_{10} \cdot 4\ Na_2Al_2Si_2O_8$. Bowen[11] maintains, on the contrary, that nephelines are responsive in composition to the magmas from which they form, those

occuring in the potash-rich rocks of one region should differ in a definite manner from those occuring in the soda-rich rocks of another region. He concludes that nepheline is made up of pure soda nepheline with a kaliophilite molecule and two plagioclase molecules, albite and anorthite, in solid solution. The composition reported is then $Na_8Al_8Si_8O_{32}$.

Bannister[12] states that the occurance of nepheline as well-formed crystals is restricted to comparatively few localities, although as the massive variety, elaeolith, and more generally as a rock-forming mineral it is very widely distributed. According to Bowen and Grieg[13] the compound $NaAlSiO_4$ is stabile below 1248°C. as a hexagonal form corresponding with nepheline and above this temperature as a triclinic form with lamellar twinning which has been called carnegieite.

Gottfried[14](1926) found as a result of his investigations on a nepheline crystal from Vesuvius that nepheline crystallizes in the hexagonal-tetaroedral system in crystal class C_6 and gave the following measurements.

a:c = 1:0.839 where

$\underline{a}$ = 10.09 A.

$\underline{c}$ = 8.49 A.

From the identity period, the molecular weight of nepheline $(SiO_4)^{Al}_{Na}$, which is 146.0 and its density, 2.60, he found

the contents of the elementary cell, V = 749 A^3., and the number of molecules in the unit cell, Z = 8.08. Hence, there are 16 molecules in the orthohexagonal unit cell, of which there are 16 Na, 16 Al, 16 Si, and 64 O atoms. The assigned space group is C_6^6 - $C6_3$.

Gossner[15](1927) disagrees with the findings of Baumhauer and states that not all of the physical properties of nepheline are in accord with placing it into the hexagonal-pyrimidal class. He claims that the dihexagonal-dipyrimidal class will give full agreement with the physical properties and that if one insists on placing nepheline in the pyrimidal class, then the space group C_6^6 - $C6_3$ is the only one giving the even orders of the (000$\underline{1}$) reflections which the x-ray data presents. Gossner, however, rules out the space group C_6^6 - $C6_3$ on the basis that the ratio of the number of atoms with individual symmetry to the number of atoms without individual symmetry is too small.

Even though the dihexagonal-dipyrimidal class is in agreement with the physical properties of nepheline, the only symmetry shown by Laue photographs is a six-fold axis, and hence this class must also be ruled out. The space group C_{6h}^2 - $C6_3/m$ of the hexagonal-dipyrimidal class does, however, agree with existing x-ray data and permits a more satisfactory arrangement of atoms than does C_6^6 - $C6_3$, and it

is to this space group which Gossner assigns nepheline. He gives as the formula for nepheline $Si_2O_5Na_2 \cdot Al_2O_3$, and gives for the parameters:

$P_{[001]}$ = c axis = 8.37 - 8.48 (Average = 8.43 $\cdot 10^{-8}$ cm.)

$P_{[010]}$ = a axis = 10.08-10.12 (Average = 10.09 $\cdot 10^{-8}$ cm.)

a:c = 1: 0.8389

Z = 4

The unit cell contains 8 Si, 8 Al, 8 Na, and 32 O atoms.

Gossner also compares nepheline with chrysoberryl and olivine, and although there is a slight similarity in axial ratios, there is no close similarity in the parameters and in the other properties of the three minerals.

Both Gottfried and Gossner discuss the various ways of arranging the atoms of the unit cell and each concludes independently that there must be 2 Si, 2 Na, 2 Al, and 8 O atoms in the special positions and 6 Si, 6 Na, 6 Al, and 24 O atoms in the general positions.

Jaeger, Westenbrink, and Van Melle[16](1927) investigated crystals of nepheline from Monte Somma and confirmed the existence of the hexagonal unit cell belonging to the space goup C_6^6 - $C6_3$, the rhomb-based cell containing 8 $NaAlSiO_4$ and having edges, a = 9.87 A. and c = 8.38 A.. In a subsequent paper[17] Jaeger confirms this earlier work by his co-workers and himself.

Schiebold[2,18](1930,1931) studied nepheline samples obtained from Parco Chigi and found the crystals to have $\underline{a}$ = 10.1 A., $\underline{c}$ = 8.51 A., where the unit cell contained 8 molecules of $NaAlSiO_4$ and belonged to the space group C_6^6 - $C6_3$. Schiebold concludes that the structure is not close-packed hexagonal, but shows a close resemblance to that of tridymite with $[SiO_4]$ and $[AlO_4]$ groups, thus explaining the usual excess of silica in nepheline. The pseudo identity period $\underline{a}'$ of nepheline = 5.05 A., and tridymite has $\underline{a}$ = 5.03 A..

Schiebold presents a suggested picture for the structure of nepheline based on the tridymite structure in which silicon and aluminum atoms are located on the special position 3-fold axes and are surrounded by oxygen atoms in tetrahedral arrangement, while alternating silicon and aluminum tetrahedra are located in the general positions and join on to the special position tetrahedra. Two Na atoms are then located one above the other (in the Z direction) either on the 6_3 or the 2-fold screw axes, and certain sodium atoms may be replaced by Ca atoms according to this picture which Schiebold presents.

Bannister and Hey[12](1931) have made the most intensive study of nepheline, investigating some ten different samples from various localities for chemical, optical, and x-ray properties. They took over forty previous chemical

analyses of nepheline made by various workers and put the results in a common form. Of the ten samples investigated, six were from Monte Somma. All samples showed hexagonal symmetry and were represented by the simple formula $NaAlSiO_4$, although the chemical analyses proved the silica content to be greater than that indicated by the simple formula and showed some potassium to be present.

The following data was reported by these workers:

$\underline{a}$ = 9.96 - 9.99 A.

$\underline{c}$ = 8.31 - 8.38 A.

$c/a_{calc.}$ = 0.835 - 0.840

$c/a_{measured}$ = 0.834 - 0.8385

Density = 2.591 - 2.647

ω = 1.5299 - 1.5461

ϵ = 1.5264 - 1.5422

$\omega - \epsilon$ = 0.0028 - 0.0037

Number of O atoms per unit cell = 31.6-32.4

Si content range, 7.99-9.03 (Aver. = 8.50)

Al	6.94-8.13	7.50
Mg	0.00-0.23	0.03
Ca	0.00-0.52	0.35
Na	5.04-7.57	6.20
K	0.22-2.57	1.25
Si Al	15.79-16.20	16.00
Σ remainder	6.91-8.61	7.60

From the above data Bannister and Hey concluded that the unit cell of nepheline may be more correctly written as $Si_{16-n}Al_n(Na,K,\frac{1}{2}Ca)_nO_{32}$, where n varies from 6.6 to 8.2.

The values of a^2c as calculated from the forty chemical analyses reported by other workers which were accompanied by density data, range between 822 and 852 A^3., while Bannister and Hey obtain values of 824-846 from their chemical analyses and values of 821.5-837 obtained from x-ray data.

The Laue symmetry was found to be C_{6h} - 6/m with a space group of C_6^6 - $C6_3$. The authors state, following that given by Schiebold, "The rhomb-based cell contains 4 SiO_2 and the structure consists of linked tetrahedra of silicon surrounded by 4 oxygen atoms. If half the silicon atoms be replaced by aluminum, the structure becomes polar. The disappearance of the vertical planes of symmetry might be explained in terms of a rotation of each tetrahedron of Si and O and Al and O atoms about the trigonal axis, but this would not account for the a dimension now being doubled (that for tridymite). A plan of the structure perpendicular to an a dimension also shows obvious gaps for the alkali atoms, but symmetry conditions are not sufficient to fix either the exact position of the oxygen or the alkali atoms.

The silicon and aluminum atoms are fixed by symmetry

on the trigonal axes and the alkali atoms are probably situated on or around hexad axes. The gaps in the structure which accomodate the alkali atoms are about the diameter of O atoms, i.e. 2.5-2.7 A., where Na = 2.0 and K = 2.6 A. respectively."

One of the specimens studied by Bannister and Hey was a sample of pseudo-nepheline from Capo di Bove near Rome having a high potassium content. The x-ray photographs of this sample were typical of the Monte Somma nepheline and showed the pseudo-nepheline to have the same axial ratios.

Eitel and his co-workers[19](1930) investigated synthetic minerals similar in composition to nepheline by optical and x-ray methods and found the nepheline-type minerals to be hexagonal, doubly refracting optically negative crystals. For the nepheline-like crystals they found $\underline{a}$ = 9.95 A. and $\underline{c}$ = 8.42 A.. Jaeger and his co-workers[16] also studied powder diagrams of synthetic nepheline preparations and found them to give patterns identical with those of natural nepheline.

More recently Nowacki[20](1942) has studied the relation between several of the silicates and has found for nepheline that it bears a close relation to β - tridymite as shown by the following:

Nepheline	β - Tridymite
a' = 5.05 A.	a = 5.03 A.
c = 8.49 A.	c = 8.22 A.
Z = 8 $Na(AlSiO_4)$	Z = 2 SiO_4
MV = 54.7 $cm.^3$	MV = 54.58 $cm.^3$
d = 2.60 $gcm.^{-3}$	d = 2.20 $gcm.^{-3}$

The space group of nepheline, C_6^6 - $C6_3$ is a sub-group of the space group of β - tridymite, D_{6h}^4 - C6/mmc.

The comparison was next carried out between nepheline and kaliophilite. Nowacki found that the difference in the cell for the two crystals pointed to a difference in structure. He pictures the rhomb-based cell of nepheline as containing tetrahedra alternating in space, every other one with its summit pointing up, the alternate tetrahedron with its summit pointing downward. The tetrahedra in the kaliophilite cell are pictured on one level as being similar in spacial positioning with the next level containing tetrahedra rotated 180° in the horizontal plane and the summits all pointing in the opposite direction.

Belov[21] reports on the structural (statistical) formula of nepheline as being similar to that of β - tridymite in which half of the SiO_4 tetrahedra are replaced by AlO_4, and he contrasts the structural data with the 'nuclear' formula derived from chemical considerations and concludes by explaining their mutual relationship.

Almost all of the more recent work on nepheline has been concerned with the massive and rock-forming varieties and not with nepheline single crystals. This work has dealt mainly with its properties, such as fluorescence, viscosity, conversion temperature, origin, petrological conditions, uses in glass manufacture, etc.. Winchell[22] attempted to solve the problem of the chemical composition of nepheline and its correlation to the physical properties, but could find no correlation.

Chapter III

EXPERIMENTAL WORK (Part I)

The analysis or determination of any crystal structure depends first of all on being able to obtain complete and accurate data. The present chapter is concerned with the methods followed and apparatus employed in fulfilling this end. Since several of the methods and some of the equipment used were purposely designed or adapted for the first time for the purpose of this investigation, they will be described in complete detail.

A. - Selecting the crystal

Since the method to be employed was to use a beam of monochromatic x-rays and a single crystal, the first task was to obtain a truely single crystal of nepheline of suitable dimensions for x-ray crystallographic analysis. This proved to be a somewhat arduous task first, because the available supply of nepheline crystals of suitable dimensions proved to be very scarce, and secondly, because most of the available supply proved to be twinned crystals.

The crystal which was finally selected for the examination was a specimen from Monte Somma, Vesuvius, obtained through Dr. Fredrick H. Pough from the American Museum of Natural History. Since the crystal proved to be

too thick for use it was necessary to carefully split off a fragment which was to be used in all the subsequent investigation.

The fragment was mounted and adjusted to a goiniometer head using a two-circle optical goiniometer for all adjustments. For the first part of the work the crystal was mounted so that it would rotate about its c-axis direction. In subsequent work the crystal was mounted with the a axis as the rotation axis.

B. - Obtaining the negatives

The experimental techniques used to obtain the x-ray negatives and analyze them closely followed those presented in X-RAY CRYSTALLOGRAPHY[23].

Rotation photographs were made about the c-axis direction and the a-axis direction. The information obtained from these photographs enabled the calculation of the dimensions of the unit cell. From this information it was possible to calculate the reciprocal lattice dimensions and consequently the settings required for making the Weissenberg photographs. Tables I - III present such data.

Table I - General Data Concerning Nepheline

$c = 8.38 \times 10^{-8}$ cm. $\quad c^* = .1837 = \lambda/c$

$a = 9.99 \times 10^{-8}$ cm. $\quad a^* = .1778 = 2\lambda/a\sqrt{3}$

$c/a = 0.8388$

Table II - Weissenberg Layer Line Settings, c-axis rotation

Layer #	$\zeta = c^*$	μ	s	cos μ	$\cos^2 \mu$	20 $\cos^2 \mu$
0	.000	0.0°	0.0mm.	1.00000	1.000	20.00 hours
1	.183	5.3	2.3	.99572	.992	19.84
2	.366	10.6	4.6	.98294	.966	19.32
3	.549	15.9	7.2	.96174	.925	18.50
4	.732	21.4	10.0	.93106	.867	17.34
5	.915	27.2	13.1	.88942	.790	15.80

Table III - Weissenberg Layer Line Settings, a-axis rotation

Layer #	$\zeta = a^*$	μ	s	cos μ	$\cos^2 \mu$	20 $\cos^2 \mu$
0	.000	0.0°	0.0mm.	1.00000	1.000	20.00 hours
1	.178	5.1	2.2	.99604	.992	19.84
2	.356	10.3	4.7	.98389	.966	19.32
3	.534	15.5	7.1	.96363	.930	18.60
4	.712	20.8	9.7	.93483	.874	17.48
5	.890	26.4	12.7	.89571	.803	16.06
6	1.068	32.3	13.2	.88862	.714	15.80

Weissenberg photographs of the various levels were then made using the Weissenberg camera with the crystal mounted first for the c-axis rotation and then for the a-axis rotation. The exposure times employed for the individual layers as calculated in the last columns of Tables II and III take into account an automatic correction for the time-Lorentz factor according to the scheme outlined by Buerger[24,25] and Klein[25], thus making it unnecessary to correct for this factor in the latter calculations.

The negative films were then processed according to the quantitative scheme to be discussed in the following section. All Weissenberg exposures were made on Eastman No-Screen X-Ray Film using copper radiation from a Machlett tube monochromatized through a rock salt monochromater, the tube being operated at 30 kv. and 15 ma..

C. - Obtaining the positives

1. Theoretical Considerations -

One of the greatest problems in analyzing crystal structures by x-ray methods up to the present time has been the determination of the intensities of the various x-ray reflections recorded on the film. Dawton[26] devised a photographic scheme for transforming the opacity of x-ray spots to transmissive spots, the resulting transmissions being directly related to the opacity which

originally occurred. Since it is more convenient and more accurate to measure transmission of light than to measure the opacity to light, it was decided to expand and modify the Dawton technique where necessary so as to be applicable to the present problem in particular, and to other problems of the same kind in general.

In order to obtain the above desired results it was necessary to devise several new pieces of apparatus and new techniques which would be both accurate and completely reproducible. They are as discussed in the following pages.

2. Actual Procedure -

The Dawton method involves finding a negative photographic material which with a particular processing technique will give a photographic curve matching that obtained from a positive photographic material also processed in some suitable manner. It is also necessary to find, as part of the procedure, a satisfactory method for transmitting the print of the negative on to the positive material; this involves finding the correct conditions of light and time of exposure in the printing process.

After considerable experimental groundwork, a set of photographic materials with the appropriate techniques for handling them were found, these giving a satisfactory photographic match as desired. The actual choice of film

materials and conditions for processing these films had been previously investigated and worked out by Mr. John Tyler (unpublished work).

Employing the results found by Mr. Tyler, it became necessary to expand and modify these so as to be put on a more permanent basis. He found that Eastman No-Screen Film developed for 8 minutes at 65°F. (for copper radiation) in Eastman D-76 developer to which .1% KBr and 1% KI solution had been added used with Eastman Commercial Orthochromatic Films developed for 3 3/4 minutes at 65°F. in Eastman DK-50 developer gave a set of matching films when exposed under certain printing conditions. It was these printing conditions which it became necessary to standardize and put on a more suitable and useable basis.

(a). The Printing Apparatus -

The printing apparatus as constructed is diagramatically illustrated in Fig. 1. It consists essentially of a light source located on a carriage capable of moving along a graduated slide, a printing frame for holding the negative and positive films, and an automatic exposure timer for controlling the time of exposure. The light source and film holder are located inside of a light tight box painted black on all surfaces.

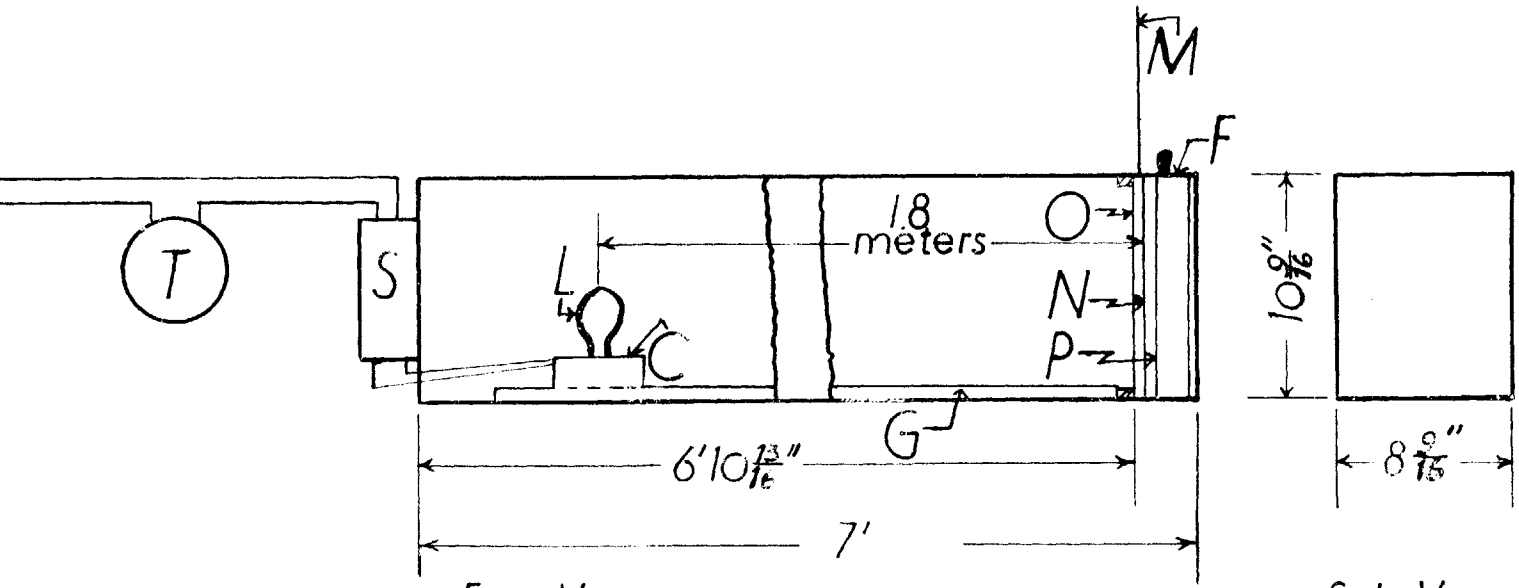

C - Movable Carriage
F - Printing Frame
G - Graduated Slide
M - Metal Slide
N - Negative Film
O - Opal Glass
P - Positive Film
S - Voltage Stabilizer
T - Timer
V - 115 volts

Note: All surfaces are painted black.

Fig. 1 - The Printing Box

The light source consists of a clear 6-watt light bulb which had been previously seasoned so as to provide a constant output. The candle power of the bulb is 3.112 horizontal candle power at a distance of 1.8 meters from the film. To aid in maintaining a constant output, the power is supplied from a 115 volt Raytheon type VR-307 voltage stabilizer. Baffles are placed at appropriate positions inside of the box to prevent light scattered or reflected from any part of the box or auxiliary equipment from reaching the film. The front of the printing frame is provided with an opal glass having a transmission filter factor of .242 so as to allow uniform illumination to fall on the film surface. In front of the opal glass there is a metal slide which enables the entire printing frame to be removed or placed in position the daylight. The automatic exposure timer is a model P-1M Reset Timer manufactured by the Industrial Timer Company.

(b). Method Used -

The negative film (which had been quantitatively processed as previously discussed in Eastman D-76 developer to which KI and KBr solutions had been added and had been developed in a tank for the appropriate time as listed in Table IV with constant agitation of the film and then fixed in Eastman X-Ray fixing solution, washed, and dried) is

Table IV - Printing Time Data

Negatives - Develop in D-76c developer for:

Copper radiation - 8 minutes

Cobalt radiation - 8 minutes

Molybdenum radiation - 6 minutes

Print for:

Copper radiation films - 18 seconds

Cobalt radiation films - 10 seconds

Molybdenum radiation films - 18 seconds

Positives - Develop in DK-50 developer for:

3 3/4 minutes for all films

---

placed in the printing frame in contact with a sheet of Eastman Commercial Orthochromatic film, and the printing frame is then dropped into its slot in the printing box. The automatic timer is then set for the correct exposure time as listed in Table IV and the exposure is made.

The film holder is then removed and the Commercial Orthochromatic film developed for 3 3/4 minutes in Eastman DK-50 developer at 65°F. with constant swabbing of the emulsion surface so as to insure uniform development. The film is then fixed in regular fixing solution (not x-ray fixer, which fails to remove the red dye base of the orthochromatic film), washed, and dried.

The above procedure was employed for all the films

for all the levels.

D. - The measurement of intensities

It was necessary to index each of the films in complete detail according to the standard practices. After each reflection had been indexed, the next problem was to measure the intensities of these spots (meaning reflections).

In order to perform the above task it became necessary to devise and build suitable equipment to do the work since no such equipment was commercially available.

(a). The Intensity Meter -

The essential parts of the intensity meter are diagramatically illustrated in Fig. 2.

The voltage which is supplied to the light source (various wattage toy-projector bulbs are used for the light source depending on the amount of illumination required) comes from a 115 volt type VR-307 Raytheon voltage stabilizer to insure uniform power output, hence uniform illumination, at all times. A General Radio Variac, type 200B, is provided in the circuit so that any level of desired brilliance may be obtained. The light beam then passes through a 3/8 inch slab of Libbey-Owens-Ford heat resisting glass frosted on both sides, which is placed in front of the light beam to insure a uniform beam and also to obsorb the heat

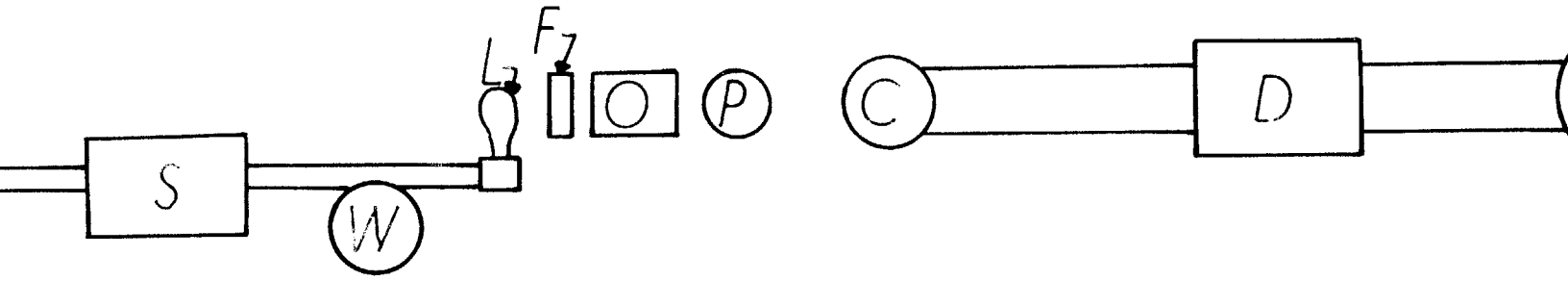

C - Photocell
D - Damping Resistance
F - Frosted Glass
L - Light Source
G - Galvanometer
O - Optical System
P - Pinhole System
S - Voltage Stabilizer
V - 115 Volts
W - Variac

Fig. 2 -Diagram of Intensity Measuring Apparatus

rays generated which might burn the film. An electric fan is placed in back of the entire system to help conduct the heat away from all parts of the system.

The lens system next converges and focuses the light beam on to the pinhole system. Interchangeable pinholes of various diameters and slits of various sizes and widths are available for use depending on the size and shape of the spot to be measured. The light then falls on the spot for which a measurement is desired and the amount of transmitted light then falls on a Weston type 3, model 594 RR Photronic Cell.

The energy falling on the photocell is next recorded on a Leeds and Northrup type R galvanometer. A critical damping resistance is in series with the galvanometer to provide for damping the galvanometer so as to give it the highest sensitivity with the lowest possible period.

In actual use the light source, lens system, Variac, and photocell are all mounted on a specially designed instrument housing (see Fig. 3). A bar, which is slotted along its upper edge, carries the film to be measured and is attached to the housing at the right in such a way that it may be raised or lowered vertically so as to move the film up or down. The front panel is sloped and the instrument built to such a height as to be convenient for anyone using the apparatus both as to ease of manipulation and

Fig. 3 - Set-up for Intensity Measurements

accessibility of observation. The photocell is mounted on a hinged arm which may be raised from the front panel to permit setting the film in its proper position.

(b). Manner of Using -

The positive film is set on the slotted bar and adjusted so that the most transmissive spot on any film of a related series is completely bathed in the light coming through the pinhole. This requires selecting a pinhole slightly larger than the largest spot on any film of the related series. The Variac is then adjusted so that the spot in question causes a galvanometer deflection which is a maximum on the galvanometer scale. This spot will hereafter be used for standardizing all subsequent films of the same series so as to put all films from the same set on a uniform basis. It is understood, of course, that once a pinhole is selected according to the above procedure, this pinhole is used for all subsequent work on the particular series of films in question.

Every spot on each film is then measured in turn. The transmission of each spot is first measured and the transmission of the film background right adjacent to the spot is then measured. The difference between the two transmissions gives the net transmission for the spot being considered.

All measurements are, of course, on a purely arbitrary

scale, but are all to the same scale for any series of films, thus rendering all readings of a series comparable. The above requirement is all that is necessary in order to obtain useable intensity data.

E. - Correcting the data

The results of the above measurements give the values for $I_{observed}$ corresponding to each reflection. These values must be corrected for Lorentz and Polarization factors. Since the Lorentz time-scale factor was taken into account in the timing of the various Weissenberg negatives it becomes unnecessary to correct for this factor.

The Lorentz-Polarization factor for the two different cases, that of the zero level and that for all levels other than zero, takes the following forms:

$$\text{Zero level} \text{ --- } \frac{1}{Lp} \approx \frac{2 \sin 2\theta}{1+\cos^2 2\theta}$$

$$\text{Levels other than zero} \text{ -- } \frac{1}{Lp} \approx \sin \Upsilon \cdot \frac{2}{1+\cos^2 2\theta}$$

Tables[25] have been published giving completely $\frac{2 \sin 2\theta}{1+\cos^2 2\theta}$ and $\frac{2}{1+\cos^2 2\theta}$ as a function of sin θ in arguments of .001 and of σ in arguments of .002. The value of σ is equal to 2 sin θ.

The vertical linear measurement, x, of any Weissenberg photograph is directly proportional to the reflection

azimuth $\mathcal{T}$, where $\mathcal{T}$ is equal to a function which is dependent on the constants of the instrument. Due to the standardization of these constants on the Weissenberg instruments, the angle $\mathcal{T}$ can be read directly in millimeters by merely measuring the vertical distance, 2x, of the spot from the center line of the film.

It is thus possible to easily calculate the correction factor for any reflection if the value of either σ or sin θ for the reflection are known. For the case of nepheline (hexagonal system) the following condition prevails:

$$\sin\theta = \sigma/2 = \sqrt{a^{*2}(h^2 + k^2 + hk) + \underline{l}^2 c^{*2}}$$

where a* and c* are the dimension of the reciprocal cell.

By means of the above, the values of sin θ and σ were calculated for each reflection (it is necessary to calculate for only one of the two, either sin θ or σ) and the corresponding value of the correct form of the Lorentz-Polarization factor was then determined from the previously mentioned tables.

The complete data and computational results are presented in the next section. Wherever possible the data from the c-axis rotation films are used. Each value of $I_{observed}$ represents an average of all the equivalent spots for the (hk$\underline{l}$) reflection in question.

F. - Experimental Data and Computations

Reflection	σ	1/L·p	I(exper.)	F^2
200	.3549	.3717	1.2	.4
300	.5329	.5903	5.3	3.1
400	.7113	.8547	1.1	.9
500	.8894	1.1681	.4	.5
600	1.0672	1.5246	.5	.8
700	1.2450	1.8653	.2	.4
900	1.6009	1.7806	1.1	2.0
10·00	1.7788	1.2177	.2	.2
12·00*				.9
110	.3081	.3191	.5	.2
210	.4706	.5099	4.6	2.3
310	.6413	.7457	.6	.4
410	.8151	1.0311	.9	.9
510	.9904	1.3654	.2	.3
710	1.3431	1.9724	.1	.2
810	1.5199	1.9294	.2	.4
910	1.6968	1.5083	.1	.2
120	.4706	.5099	1.7	.9
220	.6162	.7077	2.9	2.1
320	.7754	.9606	.7	.7
420	.9412	1.2692	.9	1.1
520	1.1109	1.6095	2.0	3.2
720	1.4560	1.9893	.1	.2
920	1.8053	1.1101	.2	.2
130	.6413	.7457	1.9	1.4
230	.7754	.9606	.1	.1
330	.9243	1.2338	.2	.2
530	1.2450	1.8563	.4	.7
830	1.7519	1.3142	.2	.3
930	1.9241	.6094	1.1	.7
140	.8151	1.0311	.2	.2
240	.9412	1.2692	.7	.9
640	1.5508	1.8829	.3	.6
740	1.7155	1.4413	.1	.1
840	1.8826	.7987	.4	.3
150	.9904	1.3654	.9	1.2
250	1.1109	1.6095	3.7	6.0
350	1.2450	1.8563	.4	.7
550	1.5405	1.8997	.4	.8
650	1.6968	1.5083	.2	.3
750	1.8571	.9001	.4	.4

* Obtainable only on films made with molybdenum radiation

Reflection	σ	1/L•p	I(exper.)	F^2
260	1.2826	1.9073	.3	.6
460	1.5508	1.8829	.3	.6
560	1.6968	1.5083	.2	.3
660	1.8485	.9416	.3	.3
170	1.3431	1.9724	.1	.2
470	1.7155	1.4413	.1	.1
570	1.8571	.9001	.4	.4
770*				1.1
180	1.5199	1.9294	.2	.4
380	1.7519	1.3142	.4	.5
480	1.8826	.7987	.4	.3
190	1.6968	1.5083	.2	.3
290	1.8053	1.1101	.2	.2
390	1.9241	.6094	1.1	.7
3•10•0*				.9

Reflection	σ	1/p	$\sin\vartheta$	I(exper.)	F^2
201	.4012	1.0840	.3600	4.1	1.6
301	.5648	1.1715	.5090	.1	.1
401	.7348	1.3040	.6704	.2	.2
501	.9083	1.4865	.7997	.8	1.0
601	1.0831	1.7091	.9056	.1	.2
701	1.2586	1.9164	.9755	.2	.4
111	.3585	1.0661	.3107	.4	.1
211	.4744	1.1186	.4617	.2	.1
311	.6670	1.2742	.6060	1.6	1.2
411	.8355	1.4053	.7385	.2	.2
511	1.0070	1.6103	.8643	.3	.4
121	.4744	1.1186	.4617	.8	.4
221	.6429	1.2267	.5906	.3	.2
321	.7967	1.3635	.7181	.3	.3
421	.9589	1.5470	.8329	.2	.3
131	.6670	1.2472	.6060	1.0	.8
231	.7967	1.3635	.7181	1.0	1.0
331	.9423	1.5274	.8171	.1	.1
431	1.0977	1.7274	.9078	.2	.3
531	1.2586	1.9164	.9736	.1	.2
731	1.5919	1.8667	.9686	.2	.4
141	.8355	1.4053	.7385	.3	.3
241	.9589	1.6129	.8329	.3	.4
341	1.0977	1.7274	.9078	.2	.3
641	1.5617	1.9077	.9796	.2	.4
841	1.8916	1.2317	.6374	.2	.2
151	1.0070	1.6103	.8643	.3	.4
351	1.2586	1.9164	.9736	.3	.6

Reflection	σ	1/p	$\sin\gamma$	I(exper.)	F^2
751	1.8663	1.4073	.6921	.2	.2
461	1.5617	1.9077	.9796	.2	.4
571	1.8663	1.4073	.6921	.1	.1
481	1.8916	1.2317	.6374	.2	.2
002	.3666	1.0692	.3599	10.4	4.0
102	.4074	1.0867	.1788	1.1	.2
202	.5113	1.1396	.3681	12.4	5.2
302	.6476	1.2314	.5314	.6	.4
402	.8002	1.3676	.6820	1.1	1.0
502	.9620	1.5521	.8100	1.3	1.6
702	1.2977	1.9516	.9803	1.4	2.7
10·02	1.8160	1.4073	.7727	.2	.2
11·02	1.9905	1.0202	.3139	.3	.1
212	.5966	1.1930	.4741	3.5	2.0
312	.7387	1.3075	.6252	.9	.7
412	.8938	1.4702	.7604	.3	.3
512	1.0559	1.6725	.8729	.3	.4
612	1.2227	1.8793	.9568	.1	.2
712	1.3921	1.9980	.9978	.2	.4
812	1.5633	1.9051	.9810	.2	.4
912	1.7361	1.5913	.8729	.2	.3
122	.5966	1.1930	.4741	.7	.4
222	.7170	1.2897	.6018	.3	.2
322	.8577	1.4292	.7314	1.5	1.6
522	1.1696	1.8188	.9324	.2	.3
722	1.5013	1.9677	.9954	.4	.8
922	1.8420	1.3468	.7385	.4	.4
132	.7387	1.3075	.6252	.3	.2
332	.9942	1.5924	.8339	.5	.7
432	1.1424	1.7841	.9212	.4	.7
532	1.2977	1.9516	.9806	.3	.6
732	1.6230	1.8155	.9563	.1	.2
932	1.9586	1.0866	.4446	.4	.2
242	1.0100	1.6129	.8453	.8	1.1
342	1.1424	1.7841	.9212	.4	.7
442	1.2857	1.9417	.9774	.1	.2
642	1.5934	1.8636	.9703	.2	.4
842	1.9178	1.1733	.5793	.4	.3
152	1.0559	1.6725	.8729	.7	1.0
252	1.1696	1.8188	.9342	1.0	1.7
352	1.2977	1.9516	.9806	.3	.6
452	1.4367	1.9980	1.0000	.5	1.0
552	1.5834	1.8783	.9744	.2	.4
752	1.8929	1.2317	.6414	.4	.3
162	1.2227	1.8793	.9568	.5	.9
262	1.3338	1.9763	.9898	.2	.4

Reflection	σ	1/p	$\sin\vartheta$	I(exper.)	F^2
462	1.5934	1.8636	.9702	.3	.5
562	1.7358	1.5913	.8695	.2	.3
662	1.8844	1.2498	.6508	.1	.1
272	1.5013	1.9677	.9954	.6	1.2
472	1.7541	1.5506	.8536	.1	.1
572	1.8929	1.2317	.6414	.4	.3
182	1.5633	1.9051	.9810	.1	.2
382	1.7897	1.4680	.8131	.1	.1
192	1.7361	1.5913	.8729	.3	.4
392	1.9586	1.0866	.4446	.4	.2
103	.5779	1.1808	.1840	.9	.2
203	.6553	1.2376	.3746	15.3	7.1
303	.7664	1.3339	.5344	.3	.2
403	.8991	1.4771	.6896	1.3	1.3
503	1.0455	1.6595	.8211	2.5	3.4
603	1.2004	1.8546	.9239	.1	.2
703	1.3609	1.9889	.9863	1.5	2.9
10·03	1.8617	1.3004	.7431	.2	.2
113	.6303	1.2177	.3206	.7	.3
213	.7238	1.2948	.4772	1.3	.6
313	.8448	1.4138	.6307	.1	.1
413	.9833	1.5795	.7627	2.2	2.6
913	1.7838	1.4819	.8387	.5	.6
10·13	1.9529	1.0994	.4818	4.2	2.2
123	.7238	1.2948	.4772	2.3	1.4
323	.9506	1.5370	.7385	.9	1.0
523	1.2394	1.8986	.9650	.1	.2
623	1.3953	1.9988	.9986	.1	.2
723	1.5563	1.9150	.9910	1.1	2.1
823	1.7205	1.6265	.9085	.4	.6
923	1.8871	1.2470	.6678	.2	.2
133	.8448	1.4138	.6307	.2	.2
233	.9506	1.5370	.7385	3.2	3.6
333	1.0756	1.6987	.8425	3.6	5.1
433	1.2137	1.8706	.9291	1.2	2.1
633	1.5149	1.9581	.9973	.3	.6
733	1.6739	1.7227	.9409	.2	.3
833	1.8360	1.3607	.7694	.9	.9
143	.9833	1.5795	.7627	1.1	1.3
343	1.2137	1.8706	.9291	.2	.3
443	1.3494	1.9845	.9829	1.4	2.7
543	1.4940	1.9736	.9993	.5	1.0
643	1.6453	1.7765	.9558	.1	.2
843	1.9611	1.0781	.4462	.3	.1
153	1.1327	1.7715	.8821	.2	.3
453	1.4940	1.9736	.9993	.5	1.0

Reflection	σ	1/p	$\sin\vartheta$	I(exper.)	F^2
553	1.6355	1.7947	.9632	.2	.3
753	1.9367	1.1339	.5417	3.0	1.8
163	1.2896	1.9451	.9593	.1	.2
363	1.5149	1.9581	.9973	.1	.2
663	1.9285	1.1513	.5635	1.5	1.0
273	1.5563	1.9150	.9910	1.1	2.1
373	1.6739	1.7227	.9409	.1	.2
573	1.9367	1.1339	.5417	2.7	1.7
283	1.7205	1.6265	.9085	.4	.6
483	1.9611	1.0781	.4462	.3	.1
293	1.8871	1.2907	.6678	.9	.7
1·10·3	1.9529	1.0994	.4818	2.5	1.3
004	.7332	1.3021	.6839	7.2	6.4
104	.7545	1.3226	.1908	.8	.2
204	.8155	1.3841	.3795	3.1	1.6
304	.9072	1.4865	.5519	1.1	.9
404	1.0281	1.6361	.7059	.9	1.0
504	1.1528	1.7966	.8368	.2	.3
604	1.2950	1.9501	.9397	.6	1.1
704	1.4450	1.9960	.9945	.3	.6
904	1.7610	1.5326	.8813	.3	.4
114	.7953	1.3635	.3305	.5	.2
214	.8671	1.4405	.4924	.8	.6
314	.9741	1.5669	.6481	.5	.5
414	1.0964	1.7274	.7880	.2	.3
514	1.2321	1.8900	.9018	.2	.3
124	.8671	1.4405	.4924	.5	.4
224	.9578	1.5470	.6239	.6	.6
424	1.1933	1.8477	.8729	.5	.8
524	1.3312	1.9747	.9578	.2	.4
724	1.6303	1.8054	.9763	.7	1.2
234	1.0672	1.6883	.7604	.5	.6
434	1.3073	1.9589	.9449	.7	1.3
144	1.0964	1.7247	.7880	.4	.4
544	1.5710	1.8947	.9338	.3	.6
744	1.8657	1.2912	.7314	.5	.5
254	1.3312	1.9747	.9578	.7	1.3
454	1.5710	1.8947	.9938	.1	.2
174	1.5300	1.9436	.9991	.2	.4
374	1.7430	1.5733	.9018	.2	.3
474	1.8657	1.2912	.7314	.3	.3
294	1.9486	1.1079	.5120	1.0	.6
205	.9834	1.5795	.3987	3.2	2.0
305	1.0607	1.6779	.5793	.2	.2
405	1.1602	1.8067	.7385	.4	.5

Reflection	σ	1/p	$\sin\varphi$	I(exper.)	F^2
505	1.2771	1.9350	.8686	.8	1.3
605	1.4068	1.9996	.9622	.2	.4
705	1.5460	1.9268	.9998	.8	1.5
115	.9669	1.5569	.3486	.4	.2
315	1.1185	1.7535	.6807	.7	.8
515	1.3494	1.9845	.9272	.3	.6
915	1.9285	1.1513	.5850	.3	.2
125	1.0305	1.6388	.5135	.4	.3
225	1.1045	1.7352	.6561	.2	.2
325	1.2004	1.8546	.7902	.4	.6
425	1.3138	1.9635	.9003	.2	.4
725	1.7205	1.6265	.9409	.4	.6
135	1.1185	1.7535	.6807	.4	.5
235	1.2004	1.8546	.7902	.9	1.3
335	1.3015	1.9547	.8894	.4	.7
435	1.4181	2.0000	.9668	.3	.6
635	1.6832	1.7027	.9659	.2	.3
735	1.8276	1.3793	.8161	.3	.3
835	1.9771	1.0447	.3714	.6	.2
245	1.3138	1.9635	.9003	.3	.5
345	1.4181	2.0000	.9668	.2	.4
445	1.5359	1.9376	.9993	.2	.4
545	1.6643	1.7425	.9748	.1	.2
645	1.8014	1.4401	.8554	.3	.4
155	1.3494	1.9845	.9272	.4	.7
355	1.5460	1.9268	.9998	.3	.6
455	1.6643	1.7425	.9748	.2	.3
655	1.9285	1.1513	.5850	.2	.1
365	1.6832	1.7027	.9659	.1	.2
275	1.7205	1.6265	.9409	.3	.5
385	1.9771	1.0447	.3714	.5	.2
006	1.1005	1.7301	.9186	4.4	7.0
106	1.1149	1.7483	.2113	.3	.1
306	1.2231	1.8815	.6046	.9	1.0
406	1.3103	1.9531	.7705	.3	.5
906	1.9424	1.1208	.5476	1.3	.6
116	1.1428	1.7841	.3616	.4	.3
216	1.1971	1.8522	.5358	.2	.2
316	1.2736	1.9312	.7071	.4	.5
416	1.3693	1.9924	.8536	.1	.2
516	1.4805	1.9822	.9553	.1	.2
816	1.8764	1.2681	.7524	.5	.5
226	1.2613	1.9205	.6820	.9	1.2
426	1.4481	1.9952	.9323	.2	.4
526	1.5636	1.9051	.9934	.6	1.1
136	1.2736	1.9312	.7071	.7	1.0

Reflection	σ	1/p	$\sin\chi$	I(exper.)	F^2
236	1.3461	1.9826	.6212	.1	.2
646	1.9016	1.2090	.6871	.4	.3
256	1.5636	1.9051	.9934	.6	1.1
356	1.6616	1.7464	.9845	.1	.2
556	1.8931	1.2271	.7096	.5	.4
166	1.5037	1.9662	.9642	.1	.2
266	1.6900	1.6903	.9823	.3	.5
466	1.9016	1.2090	.6871	.2	.2
376	1.9264	1.1557	.6102	.2	.1
207	1.3312	1.9747	.9949	.4	.8
707	1.7875	1.4725	.7944	.6	.7
217	1.3670	1.9914	.9976	.2	.4
417	1.5210	1.9522	.9877	.4	.8
727	1.9416	1.1230	.4818	2.4	1.3
337	1.5815	1.8811	.9759	.8	1.5
437	1.6793	1.7128	.9259	.4	.6
147	1.5210	1.9522	.9877	.6	1.2
447	1.7804	1.4912	.8368	1.0	1.2
547	1.8923	1.2317	.6428	.8	.6
167	1.7353	1.5935	.9232	.2	.3
008	1.4663	1.9889	.9972	.8	1.6
208	1.5100	1.9616	.9877	1.0	1.9
408	1.6310	1.8036	.9385	.4	.7
508	1.7152	1.6353	.8729	.8	1.1
608	1.8136	1.4120	.7660	.6	.6
708	1.9240	1.1601	.5180	3.8	2.3
218	1.5412	1.9321	.9823	.4	.8
318	1.6014	1.8531	.9593	.4	.7
418	1.6780	1.7147	.9121	.4	.6
518	1.7697	1.5142	.8251	1.0	1.2
228	1.5927	1.8667	.9668	.4	.7
328	1.6586	1.7501	.9397	.4	.7
528	1.8390	1.3514	.7242	2.2	2.2
628	1.9485	1.1058	.4509	1.4	.7
138	1.6014	1.8531	.9593	.8	1.4
238	1.6586	1.7501	.9397	.4	.7
438	1.8221	1.3910	.7771	1.6	1.7
538	1.9233	1.1601	.5476	.8	.5
248	1.7427	1.5756	.8780	1.0	1.4
348	1.8221	1.3910	.7771	.2	.2
158	1.7697	1.5142	.8251	.6	.8
258	1.8390	1.3514	.7242	2.4	2.5
358	1.9233	1.1601	.5476	1.6	1.0
268	1.9485	1.1058	.4509	2.2	1.2

Reflection	σ	1/p	$\sin\vartheta$	I(exper.)	F^2
419	1.8410	1.3501	.7431	.8	.6
139	1.7794	1.4935	.8406	.2	.3
439	1.9740	1.0530	.6347	1.0	.7
149	1.8410	1.3501	.7431	1.0	1.0
00·10	1.8330	1.3701	.7321	3.0	3.0
30·10	1.9089	1.1912	.5534	2.0	1.3
40·10	1.9665	1.0676	.3453	.8	.3
22·10	1.9350	1.1361	.4909	3.2	1.8
13·10	1.9431	1.1186	.4818	.8	.4

Chapter IV

EXPERIMENTAL WORK (Part II)

Chapter III was concerned with the experimental techniques, equipment, and in general with the manner in which the experimental data was obtained. The present chapter is concerned with the various manners in which this data was handled and adjusted in attempting to solve for the X and Y atomic parameters and the arguments and theory which were followed in arriving at these ends.

A. - Space group data

From the list of observed reflections presented in Chapter III, section F, it can be seen that the only systematically missing reflections (extinctions) are 0001, 0003, 0005, etc., in other words, the odd orders of(000$\underline{1}$). (In listing the reflections in that section the third index was purposely omitted in all cases as being superfluous.)

The diffraction symmetry is observable from the x-ray diffraction effects and is found to be C_{6h} - 6/m, where m is indeterminate, on the basis of Laue photographs. This places nepheline in the hexagonal system and in one of the three crystal classes, namely, C_6 - 6, C_{3h} - $\overline{6}$, or

C_{6h} - 6/m. On the basis of the etch-figure evidence of Baumhauer, however, it was unequivocably placed in the crystal class C_6 - 6.

Since nepheline belongs to the hexagonal system, the lattice type may be designated either as C or H. Since the only systematically missing reflections are the odd orders of(000$\underline{1}$), a 6_3 axis of symmetry must be present in order to account for the missing reflections. Thus, nepheline has for a diffraction symbol $6/mC6_3/-$ and belongs to the space group C_6^6 - $C6_3$ (= $H6_3$).

The list of equivalent positions associated with the space group $H6_3$ is presented in Table V. A diagram of the unit cell and the symmetry elements contained therein is illustrated in Fig. 4.

Table V - Equivalent Positions in Space Group $H6_3$

2(a)	$0,0,z;\ 0,\ 0,\ \frac{1}{2}+z$
2(b)	$\frac{1}{3},\frac{2}{3},z;\ \frac{2}{3},\ \frac{1}{3},\ \frac{1}{2}+z$
6(c)	$x,y,z:\ \bar{x},x-y,z;\ y-x,\bar{x},z;$
	$\bar{x},\bar{y},\frac{1}{2}+z;\ y,y-x,\frac{1}{2}+z;\ x-y,x,\frac{1}{2}+z$

B. - Preliminary Considerations

Since the number of formula weights per unit cell turns out to be 8 $NaAlSiO_4$, there are eight each of sodium, silicon, and aluminum atoms, and 32 oxygen atoms per cell.

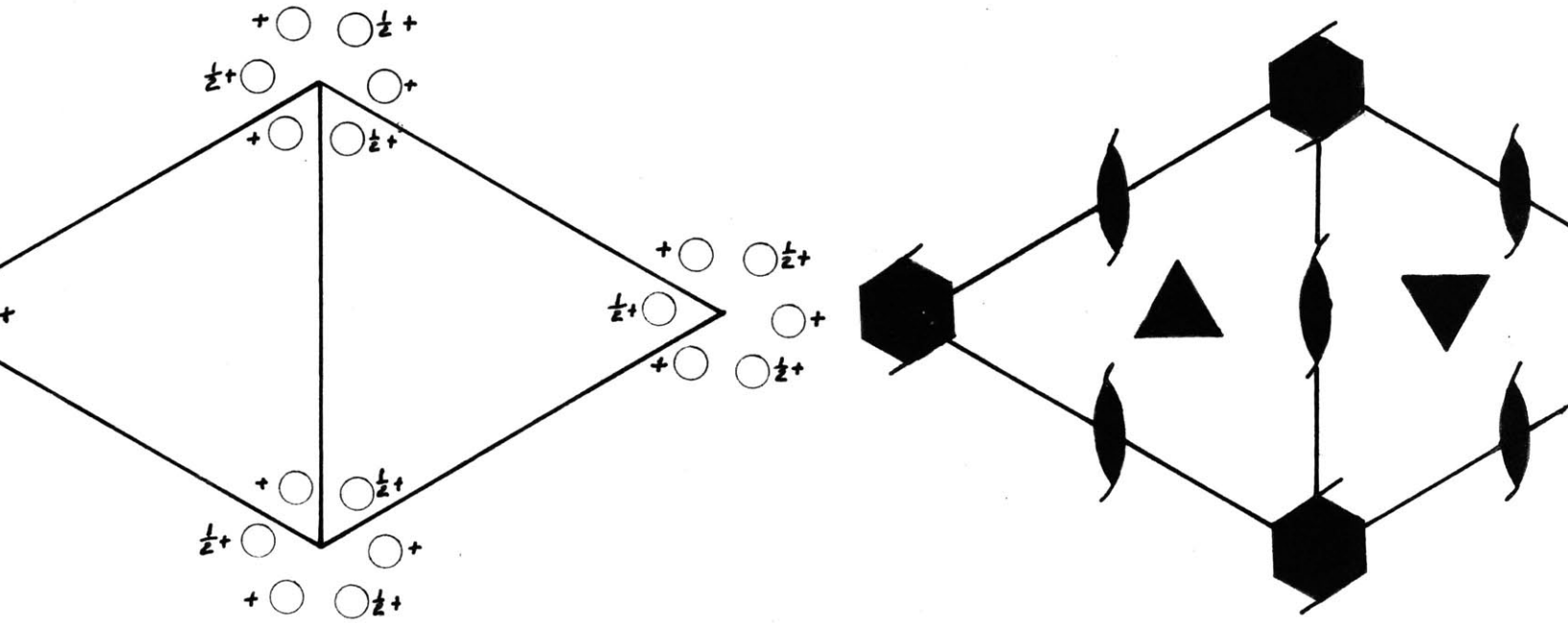

Fig.4 – Elements in Space Group $C_6^6 - C6_3$ $(H6_3)$

In order to conform to the elements of the space group, it must be concluded that there are essentially two types each of sodium, silicon, and aluminum atoms, and six types of oxygen atoms. For example, two of the eight sodium atoms are of one type and the remaining six are of the other type. If such a distinction between the atoms is made, it is found that there is one group containing six sodium atoms, one containing six aluminum, one with six silicon, and five groups with six oxygen atoms each. There are left then two each of sodium, aluminum, silicon, and oxygen atoms.

If one atom of each group of six is placed in a general position in the cell, the symmetry elements of the cell immediately account for the other five atoms of the group as being symmetry-equivalent atoms according to Table V. Thus, only one atom each of sodium, silicon, aluminum, and five oxygen atoms must be placed in general positions in the cell.

There still remain to be placed two atoms each of sodium, silicon, aluminum, and oxygen. Since according to Table V there are two sets of equivalent positions located on symmetry elements, namely, 2(a) - the 6_3 axis, and 2(b) - the 3-fold axes, these remaining atoms must be placed on symmetry elements for it is only in such positions that an atom may be located without being multiplied

by the symmetry elements. The question remains as to which of the positions the sodium atoms belong and to which ones the silicon, aluminum, and oxygen atoms belong.

Since there is but one 6_3 axis belonging to each unit cell while there are two 3-fold axes per unit cell, and since there are two each of silicon and aluminum and oxygen atoms and only two sodium atoms in all to be placed, it seems most reasonable that the two sodium atoms fall on the 6_3 axis, while one each of the silicon, aluminum, and oxygen atoms is on each of the two 3-fold axes which the space group provides. Thus, the atoms in the special positions may be readily placed as far as their positions in the XY plane are concerned.

C. - Implication Diagrams

Since a study of the Patterson plots[27,28] made from some of the very early nepheline data indicated that the Patterson plot is so complicated in the case of nepheline that analysis was impossible, no attempt was made to obtain clue as to the atomic positions from this type of diagram. The Harker synthesis[29] in its usual form did not offer any more substantial aid.

At the time that Professor Buerger introduced the concept of the implication diagram[30], the construction of such a plot gave the first clue as to the positions of some of the atoms. Harker syntheses were prepared in the

implication diagrams I3(xyO) and I6(xy$\frac{1}{2}$) employing the Patterson-Tunell method[31] for performing Fourier syntheses.

Fig. 5 presents the results of the final summations given by the Patterson-Tunell method for the case of the implication diagram I3(xyO) after the data had been transformed from the original Harker synthesis according to the rules presented in the Buerger article. The data in this plot (and in all of the following plots) is plotted to scale for the basic unit only, where the basic unit contains all of the necessary data, so that when it is operated on by the elements of symmetry which obtain to the plot in question, the entire contents of the unit cell result.

The implication diagram I3(xyO) (Fig. 6) showed several sets of peaks consisting of pairs of sharply defined peaks and pairs of bluntly defined peaks. These peaks provided several possible combinations for placing of the silicon and aluminum atoms, such as by placing a silicon atom on a sharp peak and an aluminum atom on a blunt peak, or a silicon atom on a blunt peak and an aluminum atom on a sharp peak, etc., until all of the possible permutations and combinations were tried.

The implication diagram I6(xy$\frac{1}{2}$) was prepared at a later time, and its importance and use will be discussed in the following section.

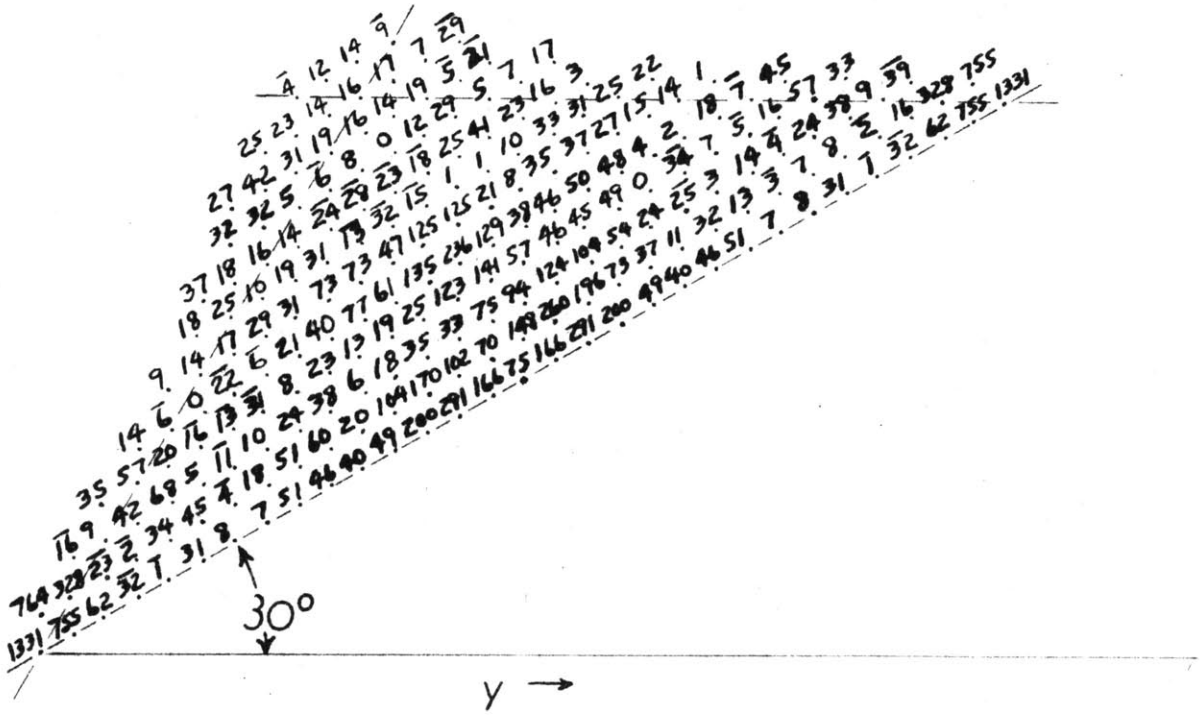

Fig. 5 – Data from Harker Implication I3 (xyO)

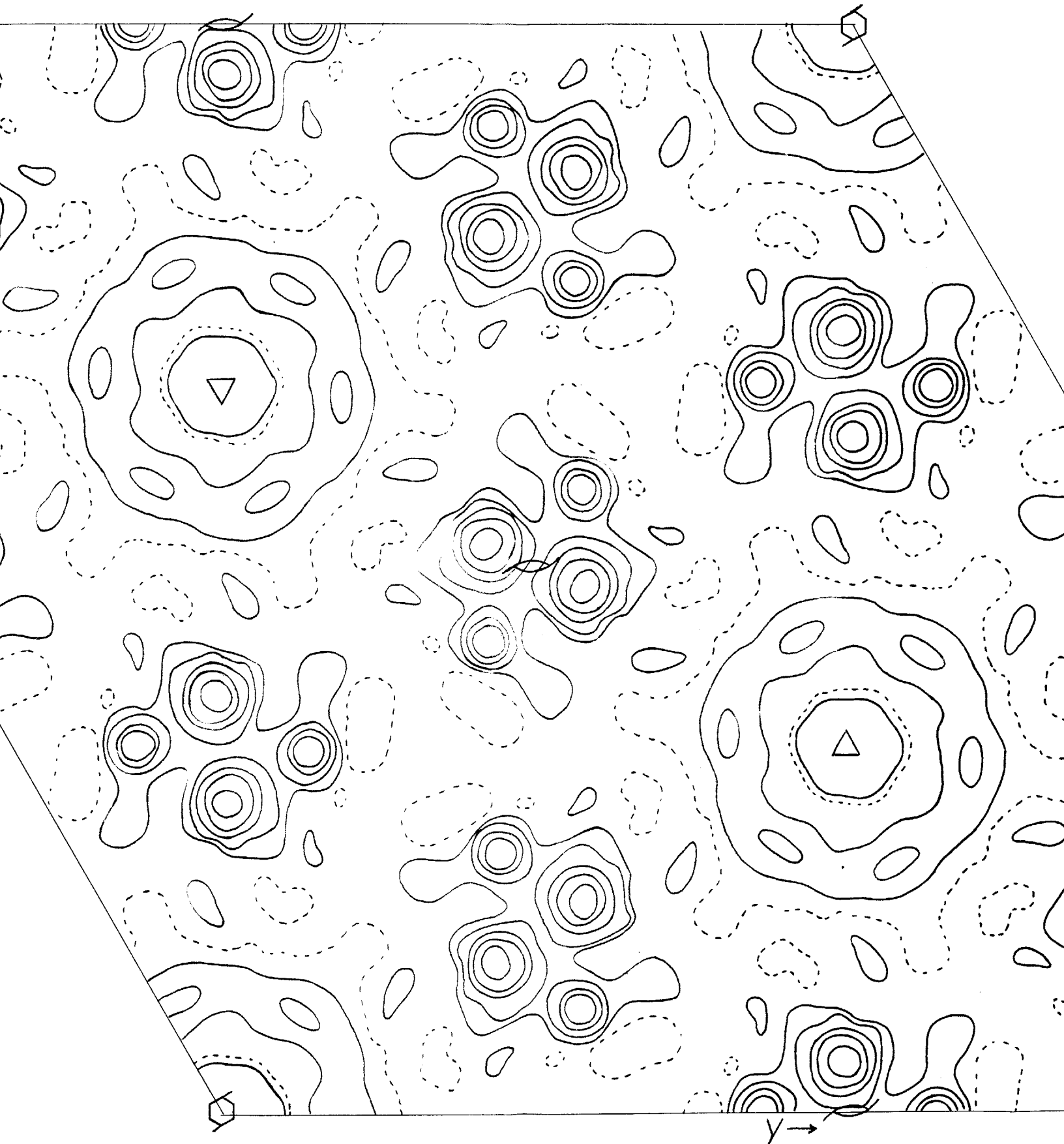

Fig. 6 —Harker Implication I3 (xyO)

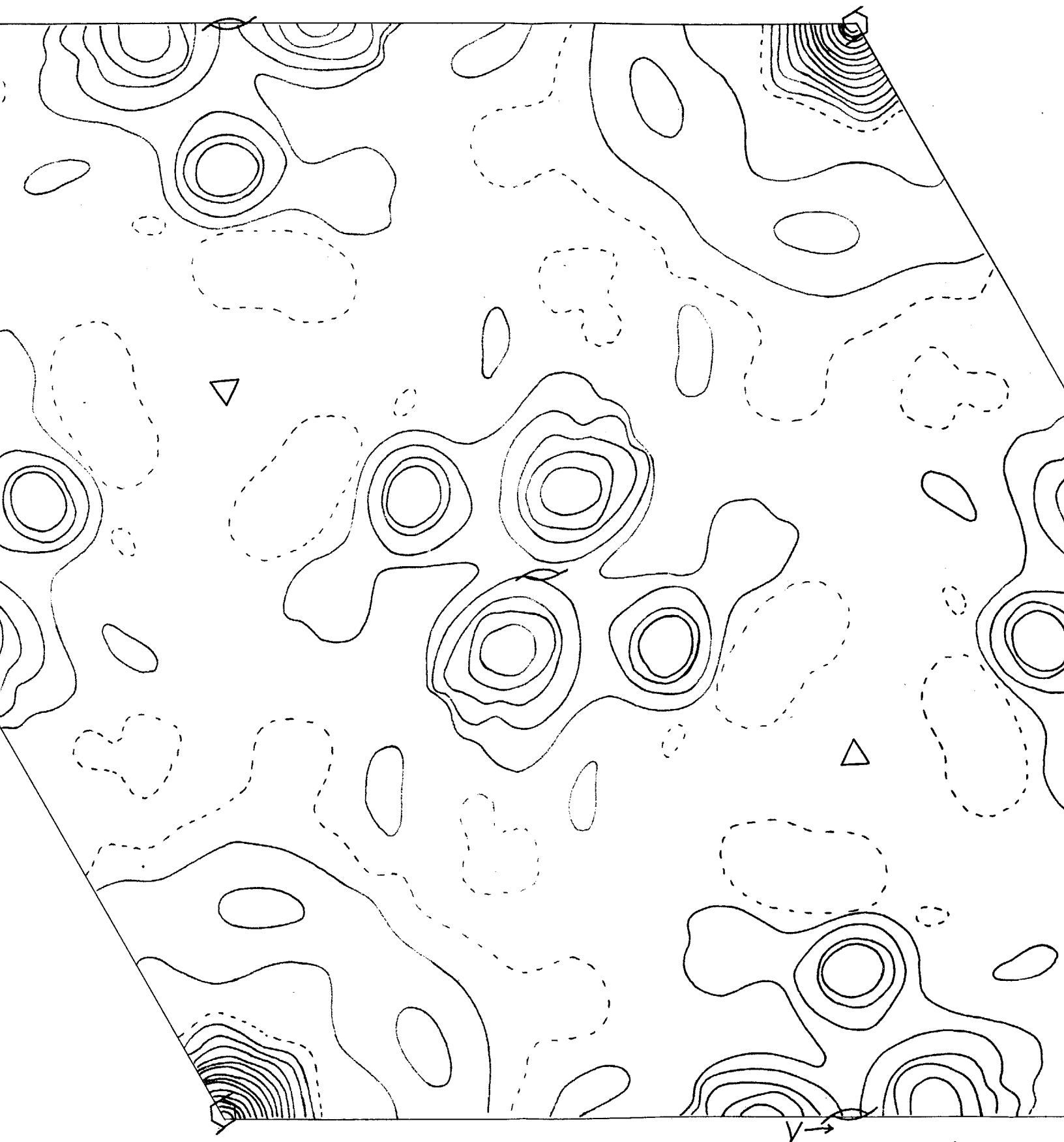

Fig.6a —Harker Synthesis P(xyO)

D. - Electron density maps

All of the possible combinations for joining the various peaks as discussed in the preceeding section were considered. For each combination an electron density plot, $\varrho(xyO)$, was prepared by using the Patterson-Tunell technique. Seventeen such plots were calculated and constructed.

Since the phases of the individual reflections could not be ascertained at this stage, it was necessary to make the assumption that the contributions of the atoms on the special positions plus those of the metal atoms, exclusive of the sodium atom, alone determine the (hkO) phases.

Such an assumption is possible since it is known from previous calculations that the combined contributions of the atoms in the fixed positions (K, Si_1, Al_1, O_1) are always either positive or very nearly equal to zero. It is possible then to conclude: a) if the net contribution of all the other atoms is highly negative, then the phase is negative; b) if the net contribution of all the other atoms is positive, then the phase is positive; and c) if the net contribution of all the other atoms is only slightly negative, then the phase is in doubt and the reflection should not be considered.

The form taken for the computation of the phases is illustrated by a sample calculation in Table VI. The theory behind the form used for the calculations will be discussed in the following section.

The various locations tried for the silicon and aluminum atoms are as listed below:

	x	y						
Si_2	.23	.33	.33	.23	.33	.23	.23	.33
Al_2	.38	.18	.18	.38	.14	.28	.28	.14
Si_2	.10	.33	.33	.10	.38	.18	.33	.23
Al_2	.28	.14	.14	.28	.14	.28	.10	.33
Si_2	.23	.33	.33	.23				
Al_2	.33	.10	.23	.33				

Each of the resulting electron density plots were studied in detail to see whether or not the peaks which resulted appeared at parameters which at least approximately coincided with the parameters which were used to obtain the phases, as illustrated in Table VI. Only two of the plots gave evidence of such coincidences. The parameters of the atoms obtained from these two plots are listed in Table VII and are designated as structures I and II.

Reflection (250) = $(25\bar{7}0)$ $\quad\quad$ $\sin\theta = .5545$

Atoms	Coordinates x	y	hx ky	Kx iy	ix hy	(1) hx+Ky	(2) Kx+iy	(3) ix+hy	(4) cos 2π(1)	(5) cos 2π(2)	(6) cos 2π(3)	∈(4)(5)(6)	√I·p f	√I +	−
K	0	0	0 0	0 0	0 0	0	0	0	1.000	1.000	1.000	3.000	3.578	10.737	
Si_1	$\frac{2}{3}$	$\frac{1}{3}$	$\frac{4}{3}\ \frac{5}{3}$	$\frac{10}{3}\ -\frac{7}{3}$	$-\frac{14}{3}\ \frac{2}{3}$	$\frac{9}{3}$	$\frac{3}{3}$	$-\frac{12}{3}$	1.000	1.000	1.000	3.000	2.832	8.507	
Al_1	$\frac{1}{3}$	$\frac{2}{3}$	$\frac{2}{3}\ \frac{10}{3}$	$\frac{5}{3}\ -\frac{14}{3}$	$-\frac{7}{3}\ \frac{4}{3}$	$\frac{12}{3}$	$-\frac{9}{3}$	$-\frac{3}{3}$	1.000	1.000	1.000	3.000	2.657	7.972	
O_1	$\frac{2}{3}$	$\frac{1}{3}$	$\frac{4}{3}\ \frac{5}{3}$	$\frac{10}{3}\ -\frac{7}{3}$	$-\frac{14}{3}\ \frac{2}{3}$	$\frac{9}{3}$	$\frac{3}{3}$	$-\frac{12}{3}$	1.000	1.000	1.000	3.000	1.171	3.512	
Si_2	.23	.33	.46 1.65	$1.15\ \bar{2}.31$	$\bar{1}.61\ .66$	1.11	$\bar{1}.16$	$\bar{.}95$	.771	.536	.951	2.258	8.507	19.208	
Al_2	.38	.18	.76 .90	$1.90\ \bar{1}.26$	$\bar{2}.66\ .36$	1.66	.64	$\bar{2}.30$	$\bar{.}536$	$\bar{.}637$	$\bar{.}309$	$\bar{1}.482$	7.972		11.814

Σ = 49.936 − 11.814
= +38.122

Table VI - Sample Phase Computations

Table VII - Atomic Parameters

	Structure I		Structure II	
Atoms	x	y	x	y
2K	0	0	0	0
$2Si_1$	1/3	2/3	1/3	2/3
$2Al_1$	2/3	1/3	2/3	1/3
$2O_1$	1/3	2/3	2/3	1/3
6Na	.62	.57	.05	.48
$6Si_2$	.24	.33	.33	.23
$6Al_2$	.38	.18	.10	.33
$6O_2$	.14	.40	.27	.24
$6O_3$	.55	.17	.50	.34
$6O_4$	.40	.52	.16	.50
$6O_5$	.28	.25	.24	.29
$6O_6$	.06	.24	.30	.05

The results as obtained from the two structures listed above still left doubt as to which one was the correct set of aluminum and silicon positions and which of the several possible positions might be used for placing of the sodium atoms. No serious attention was yet to be given to the locations of the oxygen atoms.

It was at this point that the implication diagram I6($xy\frac{1}{2}$) was introduced. A study of the diagram, Fig. 8, shows that only one set of peaks remains after applying the criterion for the elimination of non-Harker peaks. The criterion that is applicable to this particular implication is that each real Harker peak carries with it a satellitic peak of one-half the peak intensity at twice the distance from the origin as that of the real Harker peak. All non-Harker peaks do not have any such satellitic peaks associated with them.

The peaks which remained provided definite locations for the metal atoms. At the same time, only one set of peaks appeared as possible sodium locations. As a consequence of these results it was decided that structure II must be essentially the correct one.

It next became necessary to assume locations for the oxygen atoms and then recalculate the phases this time on the basis of employing the contributions due to all of the atoms. Since peaks on the electron density map corresponding to structure II suggested themselves which were in possible locations for the oxygen atoms, these were tried.

Such an electron density may was prepared, and upon examination of the peak locations which resulted it was found that not all of the resulting locations agreed with

y →

Fig.7 - Data from Harker Implication $I6(xy\frac{1}{2})$

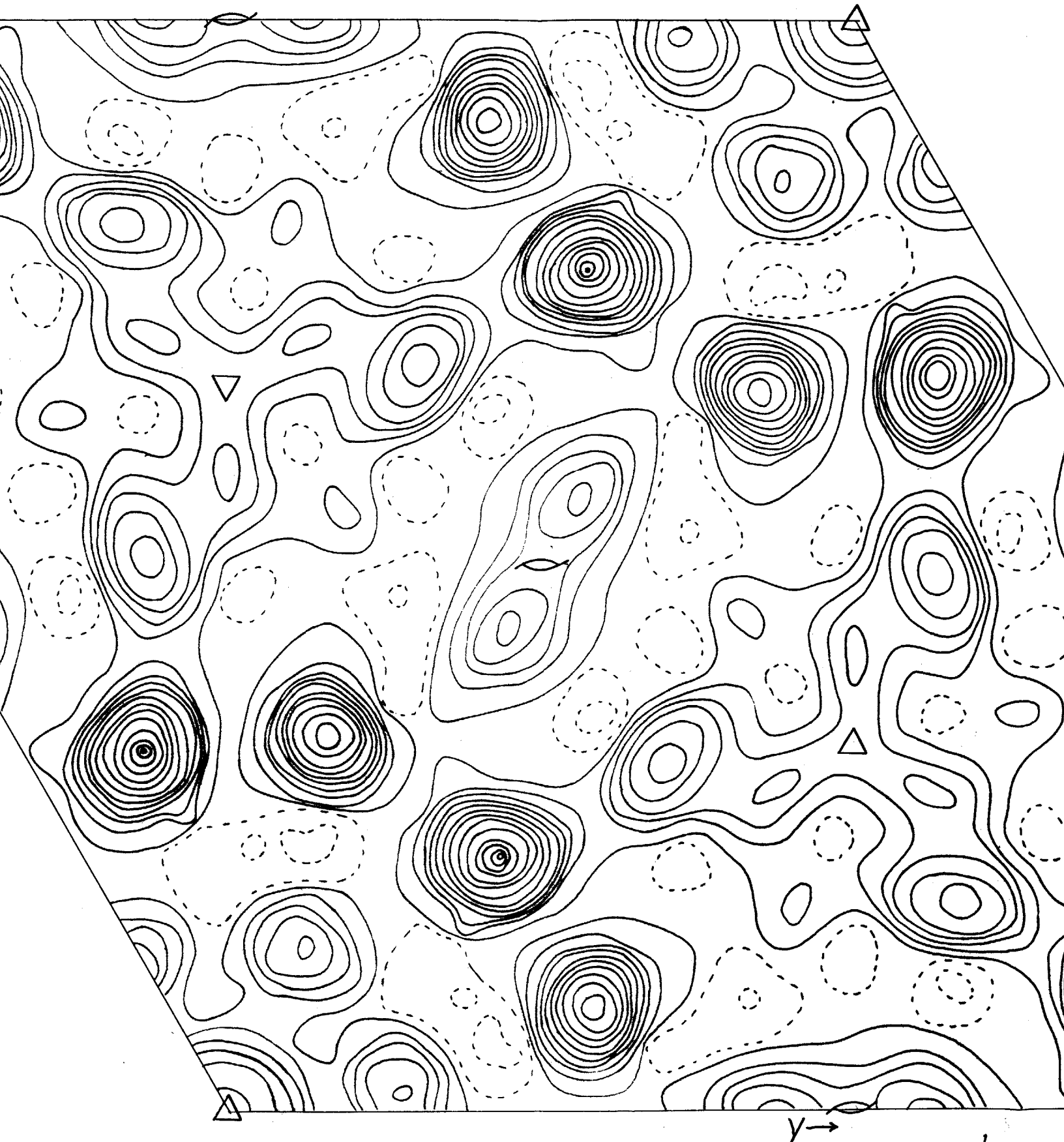

Fig. 8 —Harker Implication I6 ($xy\frac{1}{2}$)

those positions which were used in the calculations of the phases. A second set of calculations was made after adjusting those parameters which did not agree in the first trial on the basis of using the peak positions which appeared in the electron density map as the coordinates for the calculations in the succeeding trial. Once again the results showed discrepancies to exist between the parameters used for, and the parameters obtained from, the electron density map. Readjustments in positions were made and further electron density maps were prepared until finally the two sets of data were in agreement.

E. - Theoretical intensity calculations

1. Introduction -

The form taken by the structure factor for the space group C_6^6 - $C6_3$ is as follows[32]:

$$A = 2 \cos 2\pi (\underline{l}z - \underline{l}/4)\{\cos 2\pi(hx+ky+\underline{l}/4) + \cos 2\pi(kx+iy+\underline{l}/4) + \cos 2\pi(ix+hy+\underline{l}/4)\}$$

$$B = 2 \sin 2\pi (\underline{l}z - \underline{l}/4)\{\cos 2\pi(hx+ky+\underline{l}/4) + \cos 2\pi(kx+iy+\underline{l}/4) + \cos 2\pi(ix+hy+\underline{l}/4)\}$$

For those reflections having $\underline{l} = 0$, by setting $\underline{l} = 0$ and disregarding the factor 2 by which everything in the equation is multiplied, the structure factor reduces to:

$$A = \cos 2\pi (hx+ky) + \cos 2\pi (kx+iy) + \cos 2\pi (ix+hy)$$

$$B = 0$$

The calculations for the theoretical or calculated intensity values take the form discussed in NUMERICAL STRUCTURE FACTOR TABLES[33] and in the article by Buerger and Klein[34], and are presented by a sample calculation in Table VI. The following relations obtain:

For an atom in the general position -

$$I_{hkl} \propto L_{hkl} \cdot p_{hkl} |F|^2_{hkl}$$

where I = intensity of reflection

L = Lorentz factor

p = polarization factor

F = structure factor

$$I_{hkl} \propto [\sqrt{L \cdot p}\ |F|_{hkl}]^2$$

since $|F|^2 = (f_1A_1 + f_2A_2 + \ldots)^2 + (f_1B_1 + f_2B_2 + \ldots)^2$

$$I_{hkl} \propto L \cdot p \{(f_1A_1 + f_2A_2 + \ldots)^2 + (f_1B_1 + f_2B_2 + \ldots)^2\}$$

and may be written as

$$I_{hkl} \propto ([\sqrt{L \cdot p}\ f_1]_{hkl}A_1 + ([\sqrt{L \cdot p}\ f_1]_{hkl}B_1 + [\sqrt{L \cdot p}\ f_2]_{hkl}A_2' + [\sqrt{L \cdot p}\ f_2]_{hkl}B_2' + \ldots\ldots\ldots\ldots) + \ldots\ldots\ldots\ldots)$$

For all reflections where $l = 0$, the above reduces to the special expression

$$\sqrt{I_{hkl}} \propto \sqrt{L \cdot p} \cdot \Sigma f_{hkl} [\cos 2\pi (hx+ky) + \cos 2\pi (kx+iy) + \cos 2\pi (ix+hy)]_{hkl}$$

2. Application and Results -

On the basis of the electron density map for structure II which gave the most reasonable structure both from the projected interatomic distances between atoms and the coordination of the sodium atom, the metal atoms were located, namely, K at the origin (0,0), Si_1 and Al_1 at 1/3,2/3 and 2/3,1/3 respectively, Na at .008, .432, and Al_2 and Si_2 at .092, .330.

There was no doubt as to the approximate location of the Al_2 and Si_2 atoms, but it was necessary to try out several sodium locations although the region near the two-fold axis seemed the most logical place for the sodium atom from a consideration of interatomic distances and coordination of the sodium atom, and as a result of the last electron map which fed back a sodium peak at the same coordinates as were used in the calculations.

The only oxygen atom which could be placed immediately was O_1, the apical oxygen of the tetrahedron on the three-fold axis. O_2, the apical oxygen in the general position tetrahedron, O_3 and O_4, the oxygens surrounding the fixed tetrahedron, and O_5 and O_6, the oxygens surrounding the general position tetrahedron could not be easily or unmistakably placed although several regions of appropriate density suggested themselves on the electron density map.

Employing the projected interatomic distances of Al-O = 1.61 A. and Si-O = 1.51 A. respectively, the atoms O_2 and O_3 were placed at .18, .50 and .17, .53 respectively (The atom O_3 joining the silicon tetrahedron and O_4 joining the aluminum tetrahedron). The oxygen atoms O_5 and O_6 could not be resolved from one another and hence both were placed at .23, .28, the highest point on an electron density peak.

Since the position .23, .28 is not half way between the aluminum and silicon positions which O_5 and O_6 connect, an attempt was made to so split up the pair that they would be the correct interatomic distances from the respective metal atoms, but the theoretical intensity computations were definitely worsened by the process, hence both atoms were placed at the .23, .28 position.

O_2, the apical oxygen of the general position tetrahedra, was the remaining atom to be placed. Several positions of sufficient density were tried in the region of .33, .33, where another peak appears which was unaccounted for. The two positions found to be best as far as the theoretical intensity calculations are concerned were .092, .330 and .330, .330. Since the .092, .330 peak had not been occupied by any other atoms and since from a knowledge that the general position tetrahedra must be tilted in space in a manner so as to throw the apical oxygen in the

direction of .092, .330, it was decided to place this particular atom at that location. Table VIII, columns II and III presents a comparison of the calculated theoretical intensity values for the (hkO) reflections obtained by placing O_2 at the two different positions, .092, .330 (column II) and .330, .330 (column III) respectively.

Since it is known from the several analyses of nepheline made by Bannister and Hey[12] that nepheline contains more than one, but less than two atoms of potassium per unit cell on the average, it was decided to replace one potassium atom by one sodium atom in the special position. The effect of this on the intensity calculations is evident from Calumn IV of Table VIII. Calculations were also made for the case of replacing all of the potassium by sodium. This summary is presented in column V of that table. It may be observed that any attempt to replace any or all of the potassium by sodium is definitely a move in the wrong direction.

Table VIII - Comparison of Theoretical (hkO) Intensities

Note: Column I contains the listing of (hkO) reflections.

Column II contains the theoretical calculated intensities when O_2 is at .092, .330.

Column III contains the theoretical calculated intensities when O_2 is at .330, .330.

Column IV contains the theoretical calculated intensities when one K atom is replaced by one Na atom.

Column V contains the theoretical calculated intensities when both K atoms are replaced by Na atoms.

Column VI contains the observed intensities converted to a scale of the same magnitude as the theoretical calculated intensities.

I	II	III	IV	V	VI
300	100	120	115	111	100
210	82	66	71	76	92
250	98	84	81	79	83
220	79	66	62	57	74
520	87	71	68	68	61
130	64	39	35	32	61
120	68	48	43	37	57
200	53	34	41	48	48
390	67	67	65	61	44
930	45	47	45	41	44
900	45	44	43	41	44
400	30	31	28	25	44
770	64	43	42	40	39
150	40	35	37	40	39
410	37	30	28	25	39
420	30	23	21	18	39
12·00	59	58	56	55	35
240	35	29	32	34	35
3·10·0	30	35	32	30	35
320	26	19	23	25	35
310	19	29	25	23	35
600	37	39	37	35	30
110	11	16	25	33	30

I	II	III	IV	V	VI
350	41	40	38	36	26
550	35	28	26	25	26
380	32	25	24	21	26
480	29	27	25	22	26
530	24	16	18	20	26
840	18	12	15	17	26
500	15	9	12	15	26
570	11	8	11	13	26
750	1	2	1	3	26
260	30	27	25	24	22
640	28	22	20	18	22
460	28	24	23	20	22
660	19	21	19	15	23
810	26	26	25	22	17
650	27	23	21	19	17
290	25	23	21	19	17
830	24	21	22	25	17
510	19	10	8	6	17
180	19	19	21	23	17
140	17	11	8	5	17
700	15	10	12	14	17
560	13	9	11	13	17
920	13	9	12	15	17
330	9	9	6	4	17
190	7	4	6	8	17
10·00	2	1	3	5	17
710	26	19	17	16	13
910	21	20	18	16	13
230	21	19	16	13	13
470	18	14	13	10	13
740	14	13	10	8	13
170	10	8	6	5	13
720	7	10	8	6	13
620	3	2	4	5	0
450	12	14	15	16	0
360	15	8	6	4	0
100	13	2	9	21	0
270	11	9	7	5	0
440	8	7	9	10	0
820	10	8	6	5	0
11·00	10	10	14	18	0
280	8	11	9	7	0
540	7	8	7	5	0
730	6	9	7	5	0
760	5	3	6	8	0
670	4	3	6	8	0

I	II	III	IV	V	VI
800	4	3	4	6	0
340	4	6	4	2	0
430	3	3	5	7	0
1·10·0	3	3	7	11	0
630	3	10	9	7	0
610	3	2	0	2	0
370	2	0	2	3	0
160	1	0	2	4	0
10·1·0	0	0	5	9	0

As a result of the summaries presented in Table VIII it may clearly be seen that the best set of atomic x,y positions are as presented in Table IX. Fig. 10 presents the electron density projection on (xyO) obtained when the coordinates contained in Table IX are employed.

Table IX - xy Coordinates of the Atoms

	x	y
K	0	0
Si_1	1/3	2/3
Al_1	2/3	1/3
O_1	1/3	2/3
Na	.008	.432
Si_2	.092	.330
Al_2	.092	.330
O_2	.092	.330
O_3	.18	.50
O_4	.17	.53
O_5	.23	.28
O_6	.23	.28

g. 9 -Data from Electron Density Projection $\rho(xyO)$

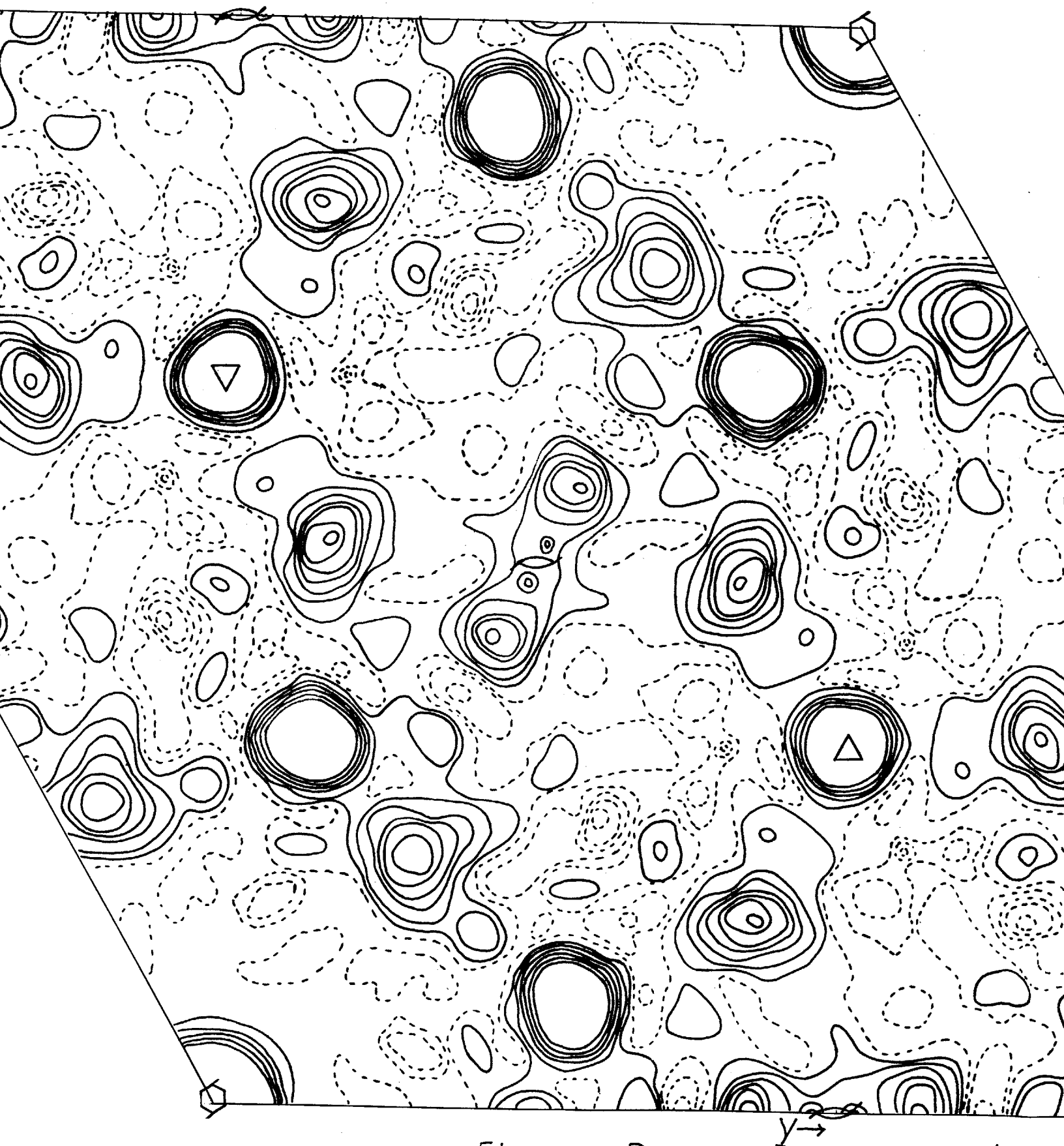

Fig.10 – Electron Density Projection ϱ(xyO

All theoretical intensity calculations were made on forms identical with that illustrated in Table VI, but with all of the atoms being included in the calculations as illustrated by the list of coordinates presented in Table IX. The parameters presented in this table do not appear as being similar to those presented in Table VII, the reason being that some of the present group have been transformed by virtue of the symmetry so as to appear in the same part of the unit cell. For example, the point 0, .33 and the point .33, 0 are symmetrically equivalent points following the relations previously presented in Table V.

As an aid in helping to determine just what effect a slight shift of any atom in a certain direction would have on the calculated intensity for any particular plane, a series of contoured structure-factor graphs as suggested by Bragg[35] and Bragg and Lipson[36] were constructed for the simpler (hk0) planes. It then became necessary only to plot the positions of the proposed atoms on a sheet of tracing paper and placing this plot in turn on top of each of the structure-factor maps. The effect on the contribution by moving any atom could thus be gained at a glance and a semi-quantitative evaluation of the amount of change could be obtained.

When it became likely that a certain shift of an

atom would generally aid a majority of the reflections, the parameters were substituted on the computation sheets and calculations were made. Since it was almost impossible to vary the positions of all of the atoms at any one time, the movement was generally handled for one atom, or at most for a pair of atoms, at one time. After much adjustment the parameters presented in Table IX were finally considered to give the best agreement between observed and calculated intensities (presented in column VI of Table VIII).

F. - Discussion of the X,Y parameters

From the results presented in Table VIII it may be concluded that only 12 of the 87 reflections are in disagreement between calculated and observed intensities for the parameters selected. No single movement or group of movements of atomic parameters will aid all of these reflections without seriously disrupting other reflections at the same time. Of the 12 "poor" reflections, three of these, (770), (12·0·0), and (3·10·0) were obtained from films made with molybdenum radiation and hence, cannot be considered too seriously as there is no direct conversion of intensities from molybdenum to copper radiation. This leaves only nine reflections which seem to be in rather serious disagreement between observed and calculated intensities.

It is not out of place at this time to point out the fact again that the atoms chosen as the basis for the calculations do not agree completely with the chemical analysis of nepheline. For example, no account has been taken of the excess of silicon over that of aluminum, of the presence of approximately .35 atoms of calcium per unit cell, and of the previously mentioned depletion of potassium. If calculations were made which accurately accounted for every atom present in the analysis (if an accurate analysis for the particular crystal used in this investigation were possible) the theoretical intensity calculations would most certainly be influenced thereby. Since such is not possible, it must be concluded that the calculated and observed data are in sufficiently close agreement to be acceptable.

To check on the accuracy of the structure as proposed for the XY plane, the method of A.D. Booth[37] was employed and R_1 was found to be equal to .34, where

$$R_1 = \frac{\Sigma_{hkl} || F_{obs.}(hkl) - F_{calc.}(hkl) ||}{\Sigma_{hkl} F_{obs.}(hkl)}$$

Booth's suggested upper limit is .20 for the substances which he studied. Since only (hk0) reflections were used in this case and the formula calls for (hkl) reflections, this cannot be considered to have too great a bearing on the accuracy of the proposed structure of nepheline at this stage of the investigation.

Chapter V

EXPERIMENTAL WORK (Part III)

Up to the present point in the determination of the structure of nepheline the only emphasis has been to locate the various atoms as far as their x and y coordinates were concerned. The positions presented in Table IX of the last chapter were considered to be as close to the exact values as could possibly be obtained from the work which had been followed.

The remaining task was to locate the atoms in the third dimension (the Z direction) and then if further evidence necessitated it, to readjust the x and y parameters on the basis of the new evidence. The contents of this chapter will describe such work.

A. - Preliminary Reasoning

Since the projection on (xyO) (Fig. 10) showed that at least in projection nepheline was based upon the tridymite structure, and since it was necessary to make some assumptions in order to start to locate the z parameters of the atoms, it was decided to place the atoms in the preliminary trials at positions where they would be found in the tridymite structure. It was realized immediately that due to the fact that the silicon and

aluminum tetrahedron on the general positions were tipped in space, that any such z values based on the tridymite structure would be ideally satisfactory, but actually incorrect even though some adjustments could easily be made from a knowledge of the metal to oxygen distances in the different tetrahedra.

An examination of Fig. 10 will show that there are two possible methods of attack for arriving at the z parameters. The first of these methods is to make a series of one-dimensional Harker syntheses, $P(x_1y_1z)$, along lines where the various atoms are located (that is, along lines perpendicular to the plane of projection of Fig. 10). The second method of attack is to make several non-centrosymmetrical planar sections of the form $\varrho(x_1y_1z)$, selecting planes which will contain several atoms each.

It may be seen from Fig. 10 that five such sections will completely cover all of the atoms. They are the planar sections $\varrho(x0z)$, $\varrho(x,2/3,z)$, $\varrho(xy0)$, $\varrho(xy\frac{1}{4})$, and $\varrho(xy\frac{1}{6})$. The three latter sections, plus the section $\varrho(xy\frac{1}{3})$ which will include some of the metal atoms in both the general and special positions, will not only tell which atoms appear at the respective z levels, but also will help to redefine the xy positions of the atoms, if such is necessary.

B. - One-dimensional Harker syntheses

A series of one-dimensional Harker syntheses was made along lines containing the metal atoms. One such synthesis was the synthesis P(1/3,2/3,z) (Fig. 11), the line (1/3,2/3,z) containing the silicon, aluminum, and apical oxygen atoms in the special positions. The other syntheses are P(.33,.23,z), P(00z), and P(.45,.45,z).

Syntheses of this type result in a curve extending along the Z direction with a series of peaks of various heights, each peak representing the distance between some atom and some other atom. Since it is known from the tridymite structure the portion of the unit cell z distance that each atom is approximately removed from some other atom, such information was used to assign which atoms belong to the various peaks.

Since each peak obtained actually represents the effect of several theoretically possible atom-atom distances, it is not possible in most cases to unequivicably assign one and only one atom-atom pair as being responsible for producing the peak. However, by observing the height of any particular peak and the various combinations which could theoretically produce the peak, it became possible to eliminate some of the combinations as being applicable to the peak in question.

Fig. 12 illustrates the projection of the idealized nepheline structure along the c axis based upon the projection

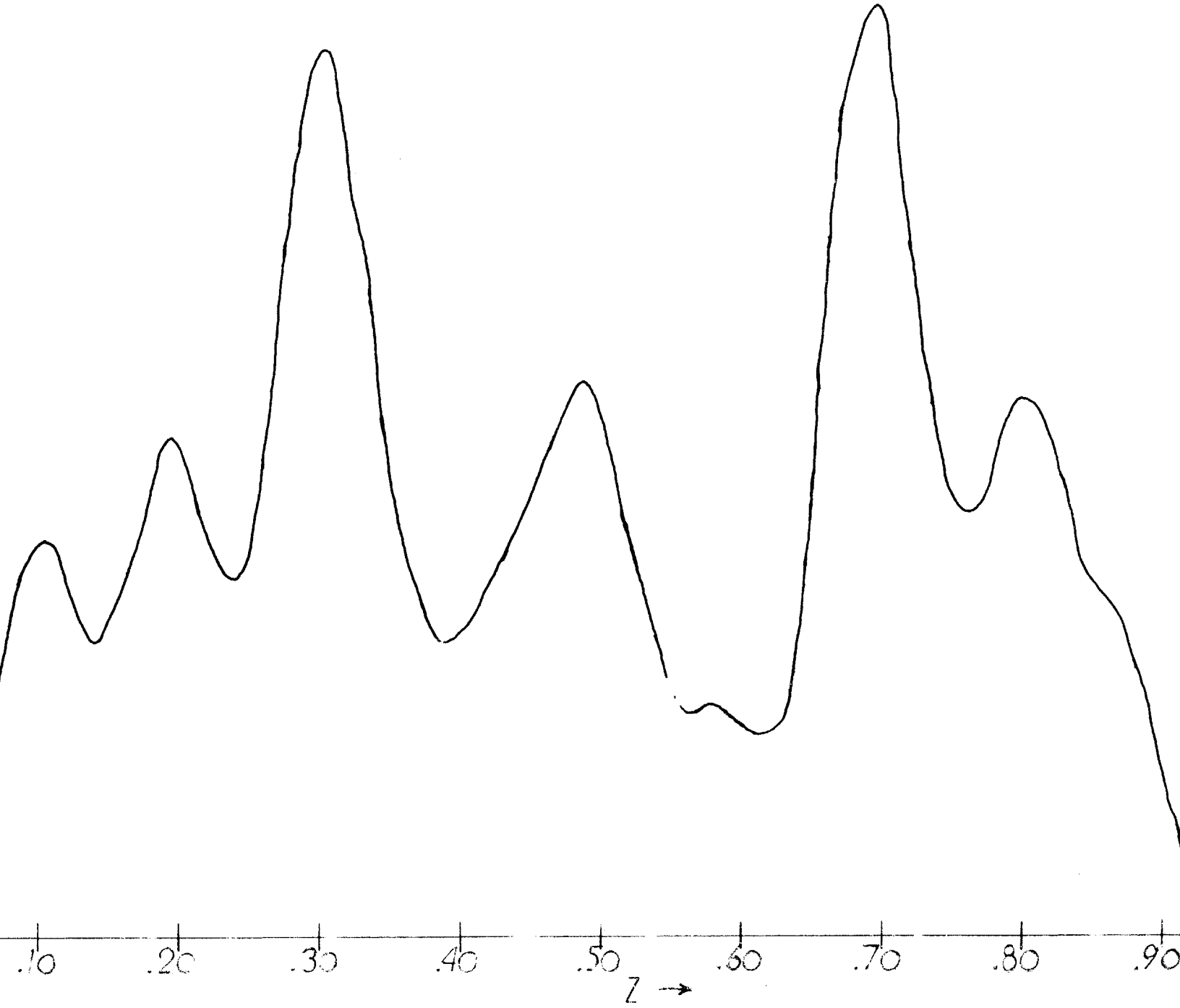

Fig. 11 - One-Dimensional Harker Projection $P(\frac{1}{3}\ \frac{2}{3}\ Z)$

of the atoms of the tridymite structure along the same axis. From this diagram it can be reasoned, for example, that the apical oxygen O_1 is at a distance of 2/12 c from an Al_1 atom and at a distance of 10/12 c from another Al_1 atom. By a similar process it is possible to determine the distance between any atom and any other atom in the Z direction.

As a result of the one-dimensional Harker syntheses, a study of Fig. 12, and the results obtained from the electron density projection to be discussed in Section D, the approximate z parameters were assigned to the atoms as follows.

Table X - Approximate z Parameters

Atom	z
K	0
Si_1	.82
Al_1	.18
O_1	0
Na	.50
Si_2	.33
Al_2	.67
O_2	.50
O_3	.75
O_4	.25
O_5	.25
O_6	.75

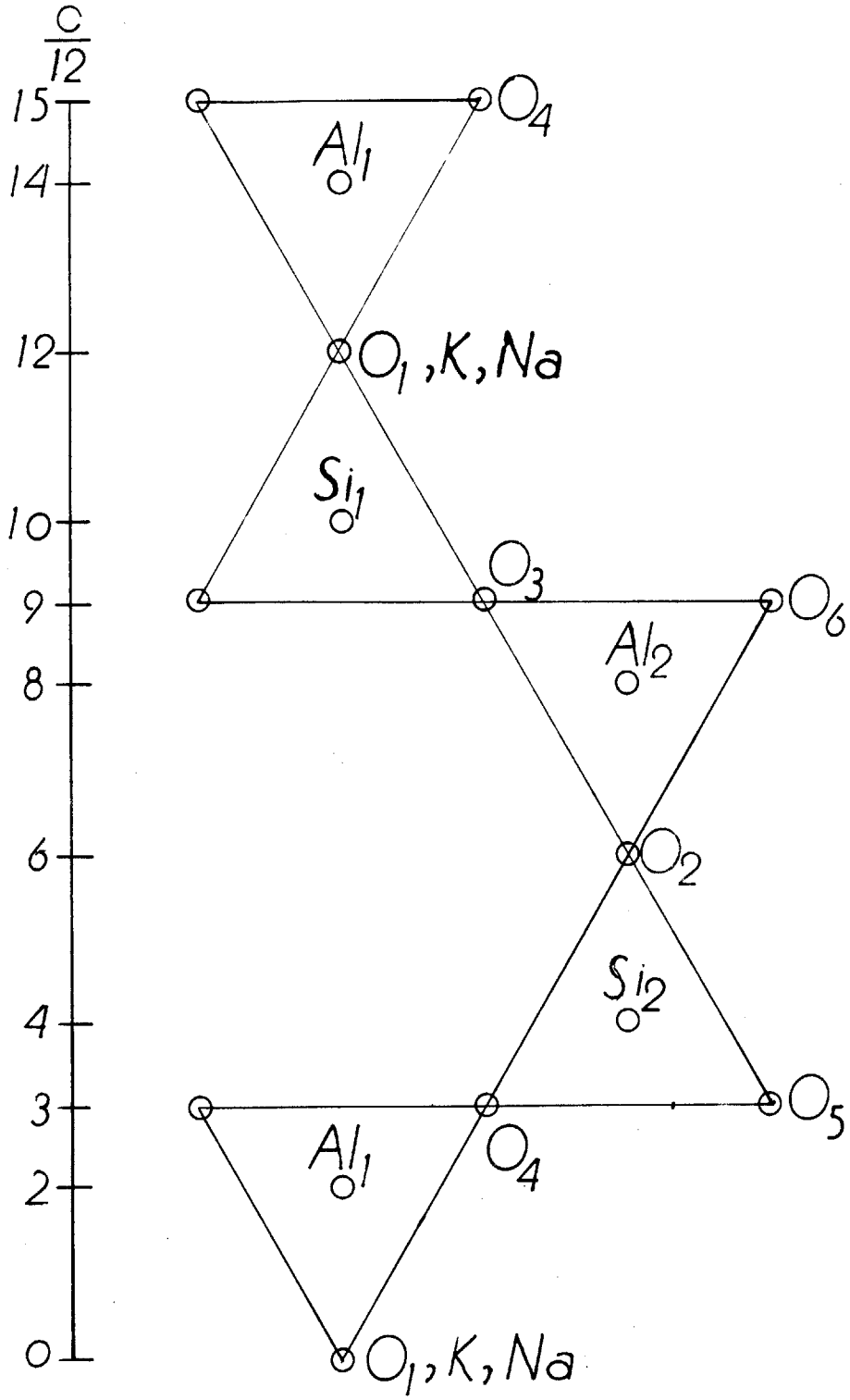

Fig 12 - Projection of Idealized Nepheline Structure Along the C Axis

C. - Calculation of structure factor components

The general form taken by the structure factor was presented in Chapter IV, Section F.

For those reflections where $\underline{l} = 2n$, the factor may be recast into the following form[32]:

$$A = 2 \cos 2\pi \underline{l}z \{\cos 2\pi(hx+ky) + \cos 2\pi(kx+iy) + \cos 2\pi(ix+hy)\}$$

$$B = 2 \sin 2\pi \underline{l}z \{\cos 2\pi(hx+ky) + \cos 2\pi(kx+iy) + \cos 2\pi(ix+hy)\}$$

For those reflections having $\underline{l} = 2n+1$, the formulas for the $\underline{A}$ and $\underline{B}$ components of the structure factor reduce to:

$$A = -2 \sin 2\pi \underline{l}z \{\sin 2\pi(hx+ky) + \sin 2\pi(kx+iy) + \sin 2\pi(ix+hy)\}$$

$$B = 2 \cos 2\pi \underline{l}z \{\sin 2\pi(hx+ky) + \sin 2\pi(kx+iy) + \sin 2\pi(ix+hy)\}$$

In all of the above formulas the factor $\underline{2}$ is a trivial constant by which everything is multiplied and consequently may be omitted.

Thus, it may be seen that the forms taken for the calculation of $\underline{A}$ and $\underline{B}$ may be divided into two groups, those having $\underline{l} = 2n$ and those having $\underline{l} = 2n+1$. Since the terms contained inside the brackets is the same for and (hk$\underline{l}$) reflection for both the $\underline{A}$ and $\underline{B}$ parts in each group, the form used for the computations may be so designed as to make use of this fact.

The computational form followed is similar to that presented in Table VI and is illustrated in Fig. 13. For those reflections having $l = 2n$, the terms within the brackets are calculated in a manner identical with that in Table VI. The summation of the terms within the brackets is then multiplied by mf, where m is the multiplicity of the atom and f is the atomic scattering factor. The addition of the contributions due to all of the various atoms gives the value for A.

A second computation sheet contains only the columns for sin $2\pi l z$, mf, and the final product. This sheet is attached to the top of the first sheet so as to coincide with the corresponding columns on the lower sheet and the products are obtained. The summation of these values gives the value for B. In place of the second sheet, the entries may be included in the same square as the corresponding entries on the original sheet as illustrated in Fig. 13.

A similar pair of computation sheets is set up for those reflections having $l = 2n \pm 1$, with the appropriate column headings thereon.

Following these forms the values of the A and B components of the structure factor were computed for all the (hkl) reflections employing the x and y parameters as presented in Table IX and the z parameters as

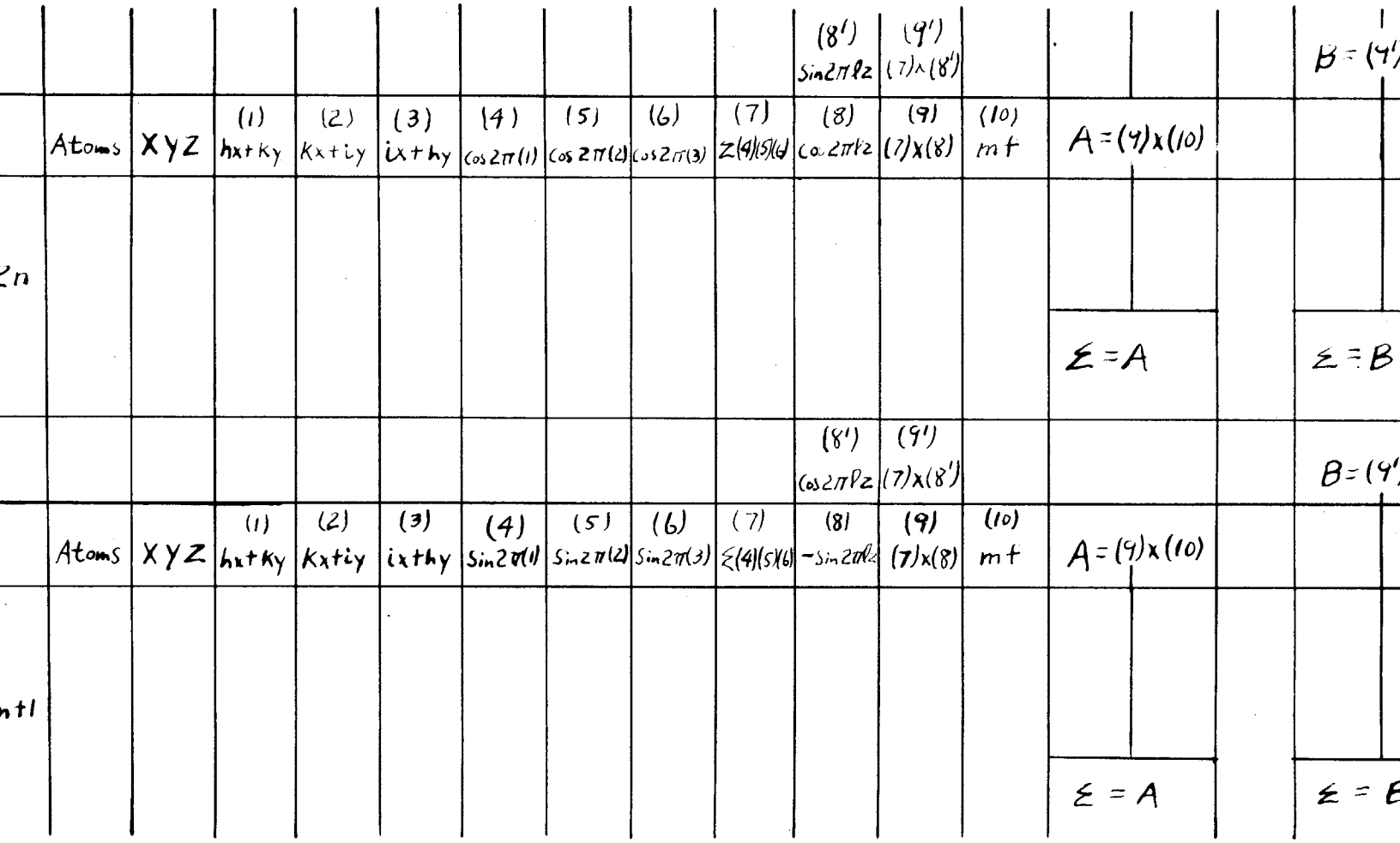

Fig. 13 - Forms for Computing A and B Components of the Structure Factor

presented in Table X.

For the purpose of performing Patterson-Tunell syntheses, however, the values of $\underline{A}$ and $\underline{B}$ are not what is demanded. The values of A_o and B_o are the desired quantities and are related to $\underline{A}$ and $\underline{B}$ as follows:

$$(1)\ A_o/B_o = A/B \quad \text{and} \quad (2)\ A_o^2 + B_o^2 = F_o^2$$

where $F_o = F_{observed}$

From (1) $A_o = B_o(A/B)$ ..... (3)

Substituting (3) in (2):

$$B_o^2 + B_o^2 (A/B)^2 = F_o^2$$

$$B_o^2(1 + (A/B)^2) = F_o^2$$

$$B_o^2 = F_o^2/(1 + (A/B)^2)$$

$$B_o^2 = F_o/\sqrt{1 + (A/B)^2}$$

Thus: $B_o = F_o/\sqrt{1 + (A/B)^2}$

$A_o = B_o(A/B)$

The values of A_o and B_o were calculated for all (hk$\underline{l}$) reflections using a value for $F_o = 10\,|F|$. This was done so as to obtain A_o and B_o values as whole numbers rather than as decimal parts as would have been the case if the actual values of $|F|$ alone were used. The only action that this has is to scale everything up by a factor of ten and makes no difference in the results one way or another. In all cases the original accuracy was maintained.

Since the values of $|F|^2$ are accurate to one decimal place to start with, the method used to obtain the value of A_o and B_o as whole numbers maintains this same degree of accuracy. Two sample calculations will illustrate the particulars.

Reflection:	(520)	(314)
	$\|F\|^2 = 3.2$	$\|F\|^2 = 0.5$
	$\|F\| = 1.5$	$\|F\| = 0.7$
	$10\|F\| = 15$	$10\|F\| = 7$
	$A_{calc.} = -33.89$	$A_{calc.} = +148.57$
	$B_{calc.} = -4.62$	$B_{calc.} = -2.27$
	$(A/B) = -33.89/-4.62$	$(A/B) = 145.57/-2.27$
	$= 7.335$	$= -65.45$
	$(A/B)^2 = 53.80$	$(A/B)^2 = 4283.70$
	$B_o = -15/\sqrt{1+54.80}$	$B_o = 7/\sqrt{1+4283.70}$
	$= -2.03 \simeq -2$	$= -.107 \simeq 0$
	$A_o = -2.03 \times 7.335$	$A_o = -.107 \times -65.45$
	$= -14.86 \simeq -15$	$= 7.003 \simeq 7$

Table XI presents the values of A_o, B_o, and $10|F|$ for all observed (hk$\underline{l}$) reflections.

Table XI - Calculated A_o and B_o Values

Reflection	A_o	B_o	10|F|
200	- 7	0	7
300	18	0	18
400	10	0	10
500	- 7	0	7
600	9	0	9
700	- 6	0	6
900	14	0	14
10·00	- 5	0	5
12·00	9	0	9
110	- 4	0	4
210	-15	0	15
310	7	0	7
410	10	0	10
510	5	0	5
710	4	0	4
810	6	0	6
910	4	0	4
120	9	0	9
220	14	0	14
320	- 8	0	8
420	11	0	11
520	18	0	18
720	4	0	4
920	- 5	0	5
130	-12	0	12
230	3	0	3
330	5	0	5
530	- 9	0	9
830	- 5	0	5
930	8	0	8
140	5	0	5
240	- 9	0	9
640	7	0	7
740	4	0	4
840	- 6	0	6
150	-11	0	11
250	24	0	24
350	9	0	9
550	9	0	9
650	5	0	5
750	6	0	6

Reflection	A_o	B_o	10|F|
260	8	0	8
460	- 7	0	7
560	- 5	0	5
660	5	0	5
170	4	0	4
470	4	0	4
570	- 6	0	6
770	11	0	11
180	- 6	0	6
380	7	0	7
480	6	0	6
190	- 5	0	5
290	5	0	5
390	8	0	8
3·10·0	- 9	0	9
201	0	-13	13
301	0	- 2	2
401	0	4	4
501	0	-10	10
601	0	- 4	4
701	0	6	6
111	0	- 4	4
211	0	- 3	3
311	0	11	11
411	0	- 5	5
511	0	6	6
121	0	- 6	6
221	0	5	5
321	0	5	5
421	0	- 5	5
131	0	9	9
231	0	-10	10
331	- 1	- 3	3
431	0	6	6
531	0	4	4
731	0	6	6
141	0	- 6	6
241	0	- 6	6
341	0	- 6	6
641	0	- 6	6
841	0	- 4	4
151	0	6	6
351	0	7	7
751	0	- 4	4
461	0	- 6	6
571	0	3	3
481	0	- 4	4

Reflection	A_o	B_o	$10\|F\|$
002	-20	0	20
102	5	0	5
202	23	0	23
302	6	0	6
402	10	1	10
502	13	0	13
702	16	0	16
10·02	5	1	5
11·02	3	0	3
212	14	0	14
312	- 9	0	9
412	- 6	0	6
512	7	- 1	7
612	4	0	4
712	- 6	0	6
812	- 6	- 1	6
912	- 5	0	5
122	- 6	0	6
222	5	0	5
322	13	0	13
522	5	- 3	6
722	9	0	9
922	6	0	6
132	- 5	0	5
332	8	0	8
432	8	0	8
532	8	0	8
732	4	0	4
932	4	0	4
242	10	0	10
342	8	0	8
442	- 3	2	4
642	- 6	- 1	6
842	5	0	5
152	10	0	10
252	-13	- 1	13
352	- 8	0	8
452	10	0	10
552	4	- 5	6
752	6	0	6
162	9	0	9
262	- 6	- 2	6
462	7	0	7
562	5	0	5
662	3	0	3
272	11	0	11
472	4	0	4

Reflection	A_o	B_o	10|F|
572	6	0	6
182	4	0	4
382	- 3	0	3
192	6	0	6
392	3	- 3	4
103	0	4	4
203	0	27	27
303	0	5	5
403	0	-11	11
503	0	18	18
603	0	4	4
703	0	-16	17
10·03	0	- 4	4
113	0	5	5
213	- 1	- 9	9
313	0	- 3	3
413	0	-16	16
913	0	8	8
10·1·3	0	15	15
123	0	12	12
323	0	-10	10
523	0	4	4
623	0	4	4
723	0	14	14
823	0	- 8	8
923	0	- 4	4
133	0	4	4
233	0	-19	19
333	0	23	23
433	0	-14	14
633	0	8	8
733	0	- 6	6
833	0	-10	10
143	0	-12	12
343	0	6	6
443	0	-17	17
543	0	-10	10
643	1	- 4	4
843	0	- 4	4
153	0	- 6	6
453	0	10	10
553	0	6	6
753	0	14	14
163	0	- 4	4
363	0	4	4
663	0	-10	10
273	0	-14	14

Reflection	A_o	B_o	$10\|F\|$
373	0	4	4
573	0	-13	13
283	0	- 8	8
483	0	4	4
293	0	9	9
1•10•3	0	11	11
004	25	0	25
104	- 4	0	4
204	13	0	13
304	9	0	9
404	10	0	10
504	5	0	5
604	10	0	10
704	8	0	8
904	6	1	6
114	5	0	5
214	8	- 2	8
314	7	0	7
414	5	0	5
514	- 6	0	6
124	- 6	2	6
224	- 8	1	8
424	- 9	1	9
524	- 6	1	6
724	11	0	11
234	8	0	8
434	11	0	11
144	6	0	6
544	7	0	7
744	7	0	7
254	11	1	11
454	4	0	4
174	6	0	6
374	5	0	5
474	5	1	5
294	8	0	8
205	0	-14	14
305	0	- 4	4
405	0	7	7
505	1	-12	12
605	0	- 6	6
705	- 1	12	12
115	0	- 5	5
315	0	9	9
515	0	7	7

Reflection	A_o	B_o	10|F|
915	0	- 4	4
125	0	- 6	6
225	0	5	5
325	0	8	8
425	0	- 6	6
725	1	- 8	8
135	0	7	7
235	0	-11	11
335	3	- 8	8
435	0	8	8
635	1	- 6	6
735	0	6	6
835	0	5	5
245	1	- 7	7
345	0	- 6	6
445	- 5	3	6
545	0	4	4
645	0	- 6	6
155	- 1	9	9
355	0	8	8
455	0	- 6	6
655	0	4	4
365	1	- 4	4
275	0	7	7
385	0	4	4
006	26	0	26
106	3	0	3
306	10	0	10
406	- 7	0	7
906	9	0	9
116	- 5	- 1	5
216	- 4	0	4
316	- 7	0	7
416	4	0	4
516	4	0	4
816	7	0	7
226	11	0	11
426	6	0	6
526	11	0	11
136	10	0	10
236	4	0	4
646	6	0	6
256	11	0	11
356	4	1	4
556	7	0	7
166	4	0	4
266	7	0	7

Reflection	A_o	B_o	10|F|
466	- 4	0	4
376	- 4	0	4
207	- 1	- 9	9
707	1	7	8
217	0	- 6	6
417	1	- 9	9
727	- 2	-11	11
337	4	-11	12
437	3	8	8
147	1	-11	11
447	10	4	11
547	1	8	8
167	1	- 5	5
008	13	- 1	13
208	14	0	14
408	8	0	8
508	11	0	11
608	8	2	8
708	15	0	15
218	9	1	9
318	8	0	8
418	7	3	8
518	-11	- 1	11
228	- 8	0	8
328	8	0	8
528	-15	- 2	15
628	8	0	8
138	- 1	5	5
238	8	0	8
438	13	0	13
538	7	1	7
248	12	1	12
348	5	0	5
158	9	1	9
258	13	- 9	16
358	10	0	10
268	-11	- 2	11
419	0	- 9	9
139	- 1	5	5
439	0	8	8
149	0	-10	10

Reflection	A_o	B_o	10|F|
00·10	-16	6	17
30·10	11	1	11
40·10	5	- 1	5
22·10	13	1	13
13·10	- 7	1	7

D. - Electron density projections

Before it became possible to arrive at the z parameters presented in Table X it was necessary to go through a series of preliminary steps of refinements. In all, a series of five electron density projections $\varrho(xOz)$ were made.

In each case the values of A_o and B_o were calculated for the 62 (h0l) reflections according to the method presented in Section C. The x parameters used were those presented in Table IX, while the z values

Table XII - z Parameters used in Electron Density Projections

Atom	z Parameters			
	I	II	III	IV
K	0	0	0	0
Si_1	.83	.80	.82	.82
Al_1	.17	.20	.18	.18
O_1	0	--	0	0
Na	0	-.01	.50	.50
Si_2	.33	.29	.33	.33
Al_2	.67	.68	.67	.67
O_2	.50	.53	.50	.50
O_3	.25	--	.75	--
O_4	.25	--	.25	--
O_5	.75	--	.25	--
O_6	.75	--	.75	--

chosen for the first projection were as listed in Column I in Table XII. The z coordinates which resulted from the synthesis are presented in Column II.

Readjustments were made in the z parameters on the basis of the results, the values of A_o and B_o were recalculated for the (h0l) reflections and a second, third, fourth, and fifth projection were made. Each time the z parameter was adjusted on the basis of the knowledge gained from the previous projection. In the last trial the parameters which resulted agreed completely with those used in the calculations as illustrated by columns III and IV of Table XII (column III contains the parameters used in the calculations and column IV contains the parameters which resulted.

No resolved peaks of sufficient height appeared to correspond to the atoms O_3, O_4, O_5, and O_6 in any of the projections, nor did any peaks other than those for which data is presented in Table XII appear. Hence, it is not possible to comment concerning the positions of these atoms and it was necessary to assume that they were correctly placed but did not have sufficient electron density to show up.

Fig. 15 presents the synthesis for the electron density projection $\varrho(x_1 2x_1 z)$, where the plane of the projection $(1\bar{2}10)$ goes through the origin and the metal and

Fig. 14 – Data from Electron Density Projection $\varrho(x, 2x, z)$

Projected on $(1\bar{2}10)$

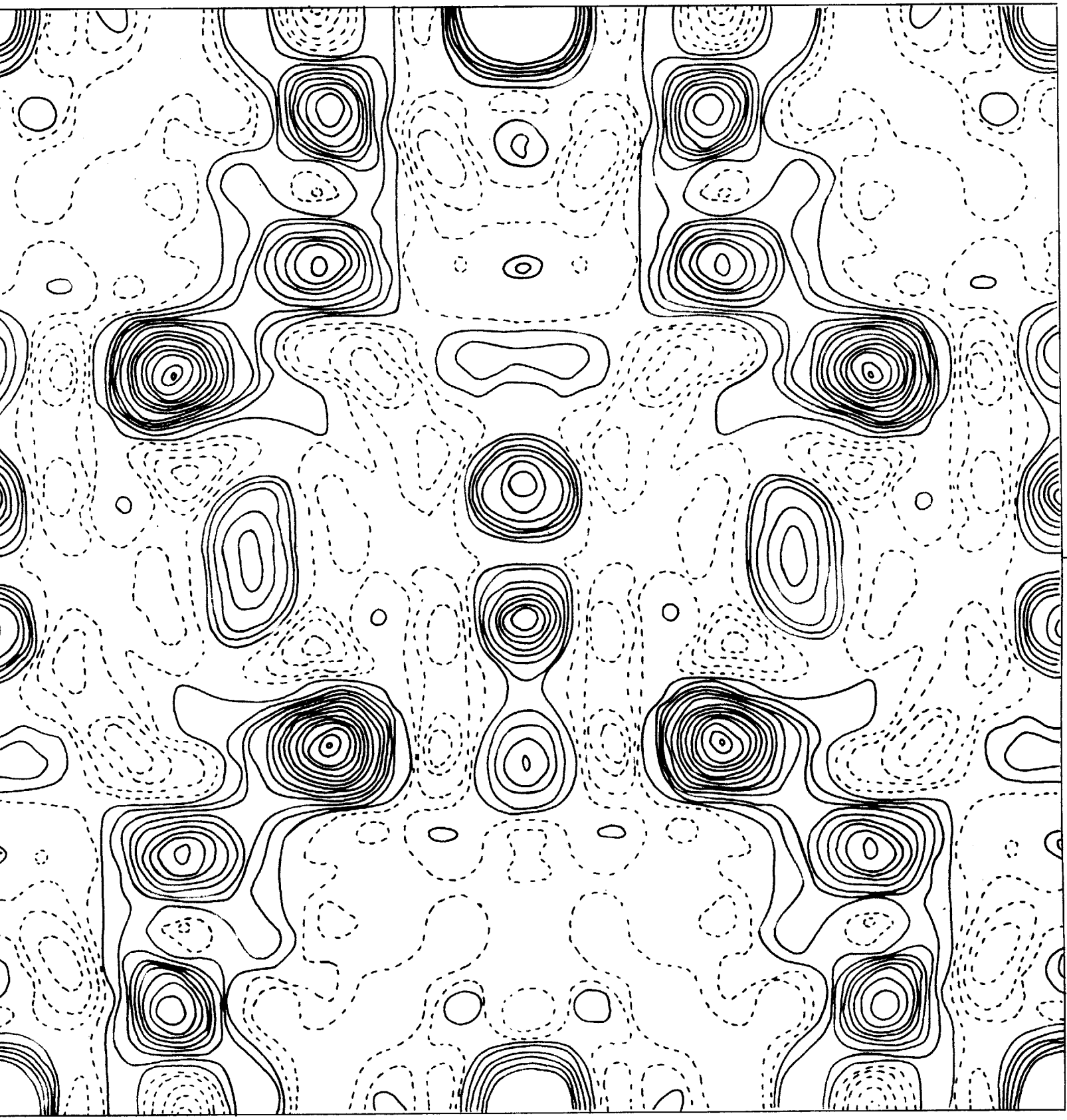
← N

oxygen atoms in the special position in the unit cell as illustrated below.

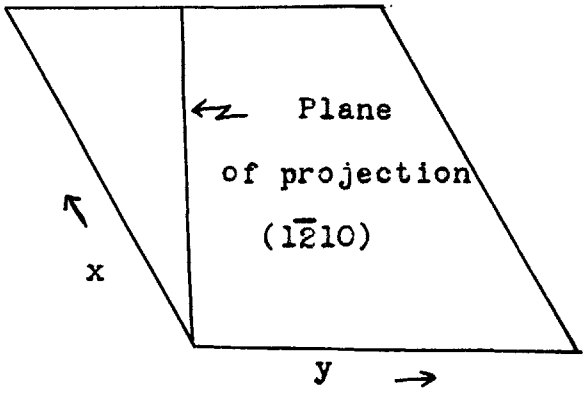

E. - Planar sections

As previously mentioned, a series of non-centrosymmetrical planar sections would give definite knowledge as to the z parameters of the atoms as well as helping to redefine the x and y parameters. The section $\varrho(xOz)$ should theoretically contain peaks corresponding to the positions of the potassium atoms, the sodium atoms, and the apical oxygen atom in the general position tetrahedron, as well as the non-apical oxygen atoms, O_5 and O_6, as illustrated in Fig. 16.

If the parameters of the atoms are placed in each of the equivalent positions in space group $H6_3$ listed in Table V, the total number of equivalent parameters are as listed in Table XIII. Fig. 16 and the corresponding illustrations of the expected atom positions for the other sections were made by employing the parameters listed in this table.

Calculations for the section $\varrho(xy0)$ would be expected to show peaks which appear corresponding to all of the atoms which have their z parameters equal to zero. As may be seen from a study of Fig. 17 (the expected atom positions in the $\varrho(xy0)$ section), the atoms which are expected to appear in this section are the apical oxygen atoms in both the special and general tetrahedron, as well as the potassium and sodium atom locations. Thus, the purpose of making this section is to verify the locations of the potassium and sodium atoms in all three dimensions and the locations of the apical oxygen atoms.

The section $\varrho(xy\frac{1}{4})$ contains all of the non-apical oxygen atoms. The expected atomic positions in this section are illustrated in Fig. 18.

The expected atom positions for the section $\varrho(x,2/3,z)$ are presented in Fig. 19. As may be seen from the illustration, both apical oxygen atoms are theoretically to be found in this section as well as the

Table XIII - Equivalent Parameters of the Atoms

oordinates	K	Si_1	Al_1	O_1	Na
, y, z	0, 0, 0	.33,.67,.82	.33,.67,.19	.33,.67, 0	.43,.43,.50
,x-y,z					.57, 0 ,.50
-x,$\bar{x}$,z					0 ,.57,.50
,$\bar{y}$,$\frac{1}{2}$+z	0, 0,.50	.67,.33,.32	.67,.33,.69	.67,.33,.50	.57,.57, 0
,y-x,$\frac{1}{2}$+z					.43, 0 , 0
-y,x,$\frac{1}{2}$+z					0 ,.43, 0

	Si_2	Al_2	O_2	O_3,O_4*	O_5,O_6*
, y, z	.09,.33,.33	.09,.33,.67	0 ,.33,.50	.17,.52,.25	.25,.28,.25
,x-y,z	.67,.76,.33	.67,.76,.67	.67,.67,.50	.48,.65,.25	.72,.97,.25
-x,$\bar{x}$,z	.24,.91,.33	.24,.91,.67	.33, 0 ,.50	.35,.83,.25	.03,.75,.25
,$\bar{y}$,$\frac{1}{2}$+z	.91,.67,.83	.91,.67,.17	0 ,.67, 0	.83,.48,.75	.75,.72,.75
,y-x,$\frac{1}{2}$+z	.33,.24,.83	.33,.24,.17	.33,.33, 0	.52,.35,.75	.28,.03,.75
-y,x,$\frac{1}{2}$+z	.76,.09,.83	.76,.09,.17	.67, 0 , 0	.65,.17,.75	.97,.25,.75

O_3 and O_4 have Z parameters differing by .50. Also, O_5 and O_6 differ by .50. The Z values presented are for the O_3 and O_5 atoms.

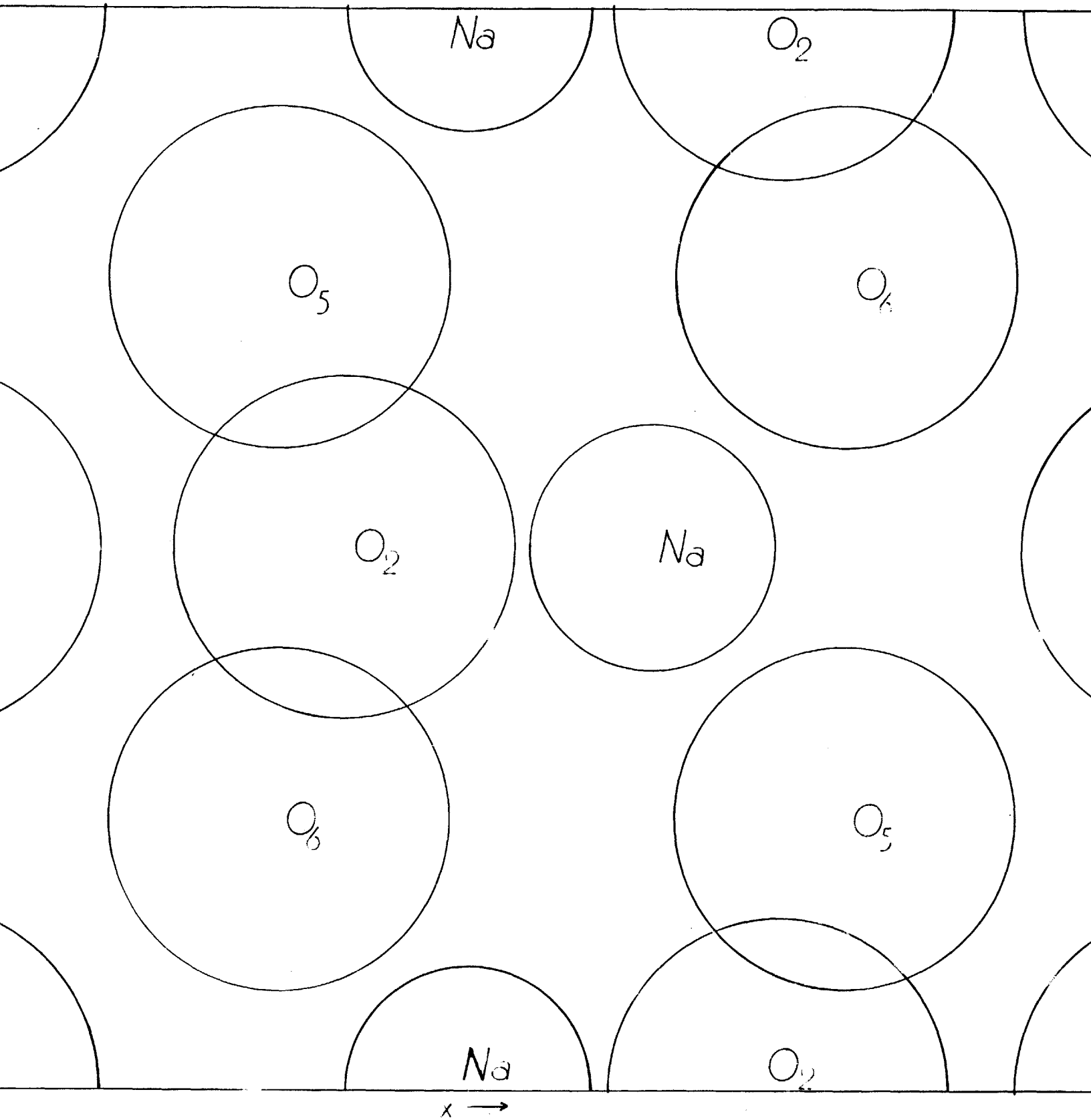

Fig.16 - Expected Atomic Positions in $\varrho(xOz)$ Section

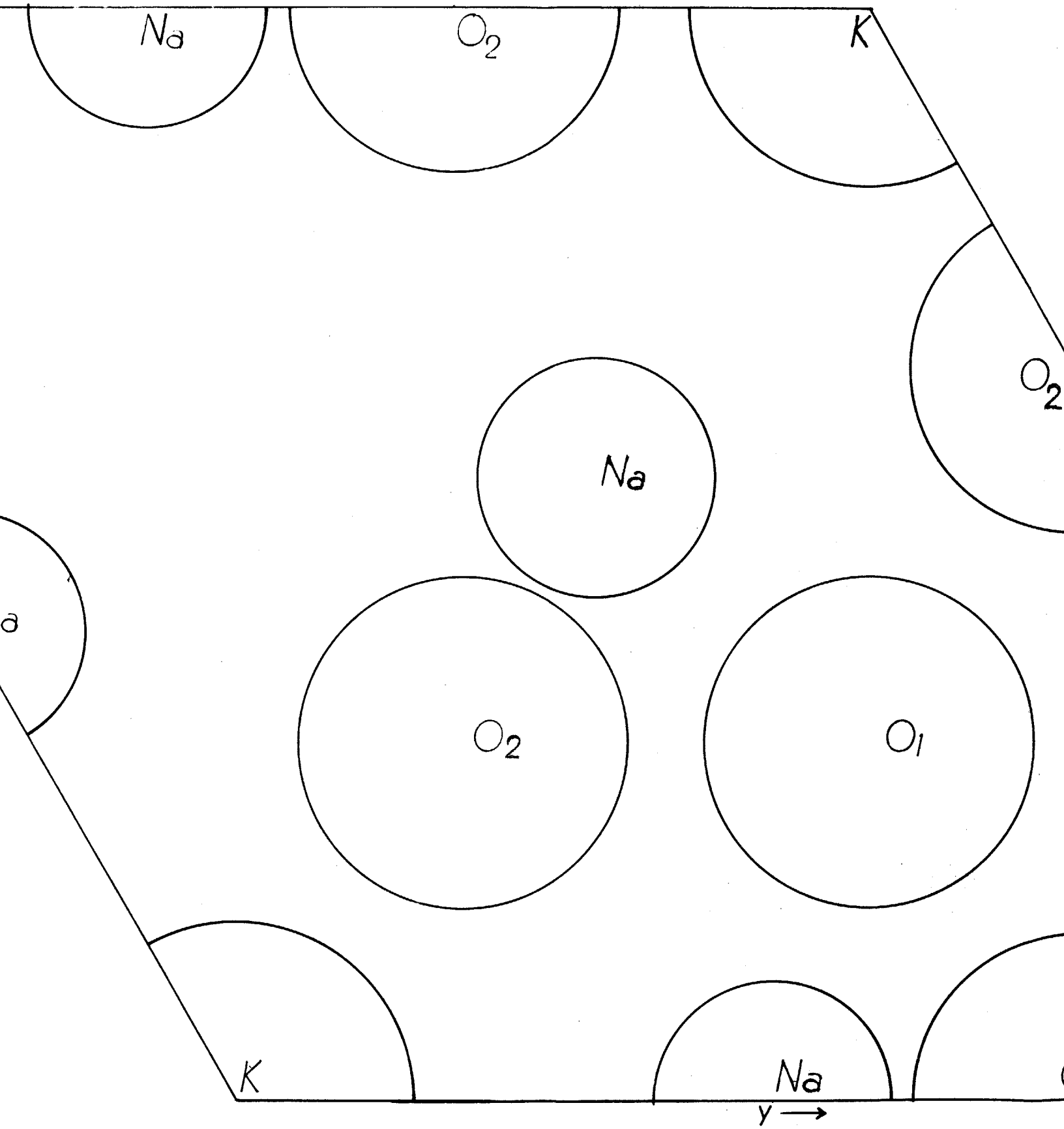

Fig 17 -Expected Atomic Positions in ϱ(xyO) Section

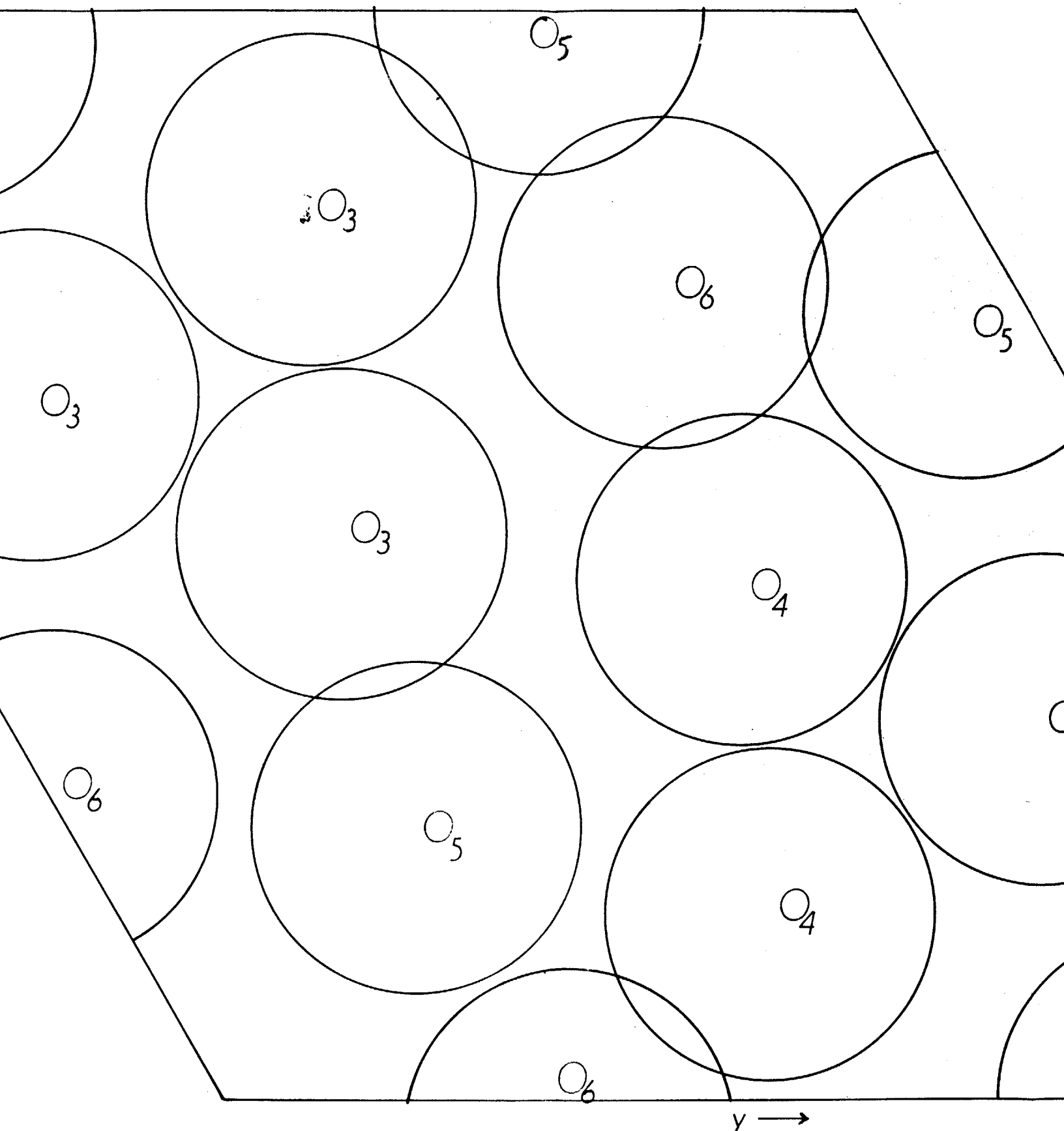

Fig. 18 - Expected Atomic Positions in $\rho(xy\frac{1}{4})$ Section

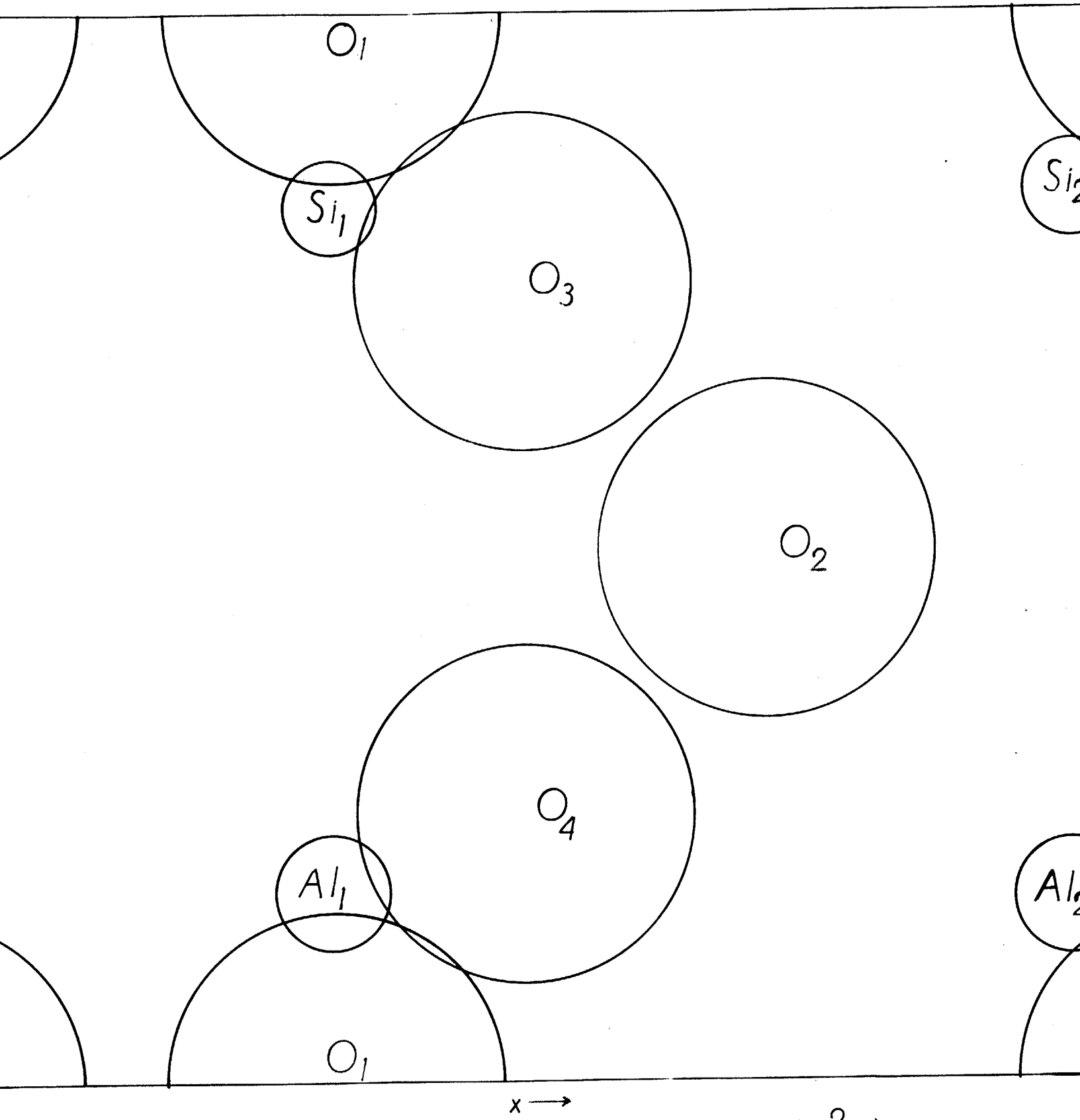

Fig. 19 -Expected Atomic Positions in $\varrho\,(x\,\frac{2}{3}z)$ Section

aluminum and silicon atoms in both the general and special positions and the O_3 and O_4 oxygen atoms.

The sections ϱ(xyl/6) and ϱ(xyl/3) should provide information concerning the locations of the aluminum and silicon atoms in both the general and special positions, these being the remaining positions about which information is required.

Chapter VI

DISCUSSION OF RESULTS

The work which has been reported in Chapters IV and V was of such a nature as to locate the three parameters of each of the atoms. It is almost certain that the x and y parameters as presented are as close to the true values as can possibly be obtained.

A study of the Harker Implication I3(xyO) and the Harker synthesis P(xyO) shows that the peaks due to both alkali atoms, sodium and potassium, and those due to all of the metal atoms coincide exactly in both syntheses. This is further exemplified by the further coincidence of the peaks in the Harker Implication I6($xy\frac{1}{2}$) with those of the previously mentioned syntheses. The conclusion to be drawn from this is that all of the metal positions are definitely located as to their x and y positions.

The incompleteness of the planar sections makes it impossible to definitely state the final z values for the atoms, but the results of the $\varrho(x_1 2x_1 z)$ projection and a knowledge of unfinished work which has been done on the sections makes it appear likely that the z parameters as stated in Table X are very close to the true values.

On the basis of the work which has been done up to the present time, the final parameters which can be

assigned to the various atoms are as listed in Table XIV.

Table XIV - Final Atom Parameters

		x	y	z
K	in 2a:	0	0	0
Si_1	in 2b:	1/3	2/3	.82
Al_1	in 2b:	2/3	1/3	.18
O_1	in 2b:	1/3	2/3	0
Na	in 6c:	.008	.432	.50
Si_2	in 6c:	.092	.330	.33
Al_2	in 6c:	.092	.330	.67
O_2	in 6c:	.092	.330	.50
O_3	in 6c:	.18	.50	.75
O_4	in 6c:	.17	.53	.25
O_5	in 6c:	.23	.28	.25
O_6	in 6c:	.23	.28	.75

The structure of nepheline proves to be based upon the tridymite framework, with NaAl substituted for half of the silicon atoms, as originally predicted by Schiebold. The chemical analyses of nepheline bear out the view that two of the eight alkali atoms are potassium and not sodium. This fact is also supported by the calculations of the theoretical intensity values as presented in Table VIII, where attempts were unsuccessfully made to replace all or

part of the potassium by sodium.

The potassium atoms occupy large holes and the sodium atoms occupy smaller holes produced by the collapse of voids in the tridymite framework so as to surround these alkali atoms. This means that the silicon and aluminum tetrahedron in the general positions are tilted in space so as to provide this collapse of the voids.

The interpretation of the region about the 3-fold axes of the Harker Implication I6($xy\frac{1}{2}$) is that the atoms of the 3-fold axes are in motion and that the parameters as presented for these atoms are in actuality only the average position assumed by these atoms. Further evidence of this fact is to be expected from the $\varrho(xy0)$ section in which case the region around the 3-fold axes would indicate that the apical oxygen atom in the special position is in motion, and from the sections $\varrho(xy1/3)$ and $\varrho(xy1/6)$ in which case evidence might be forthcoming to show that the metal atoms in the special positions are in motion about the 3-fold axes.

Such findings would be in accord with the statements of Barth[38] concerning rotational motion of the atoms in high cristobalite where he found that in the case of oxygen ions that do not lie on a straight line between two silicon ions, the oxygen ions are rotating about the line between the silicon ions.

Due to the previously mentioned fact that two of the alkali atoms are potassium atoms and not sodium atoms, the formula of nepheline is actually $KNa_3Al_4Si_4O_{16}$ and not $NaAlSiO_4$ as is generally reported in the literature and in textbooks.

Note:

All of the syntheses have been arranged to correspond to a left-handed coordinate system instead of the conventional crystallographic right-handed system. It became necessary to do this in order to maintain a uniform coordinate system for all of the syntheses since the earlier syntheses were adjusted to a left-handed system for the purpose of ease of plotting.

This, however, in no way changes the actual values for the parameters of the atoms as presented, but must be kept in mind only when viewing the illustrations.

APPENDIX

COMPUTATIONAL FORMS AND DATA USED FOR PERFORMING THE VARIOUS FOURIER SYNTHESES

A. - Introduction

As previously mentioned in the text, all of the syntheses were performed by means of the Patterson-Tunell method. The actual form for placing the data on paper differs somewhat from that suggested by the original authors and proved much more useful and convenient*. It consists of a form, Table 1 in Fig. A1, on which are placed the actual data to be used in the synthesis and contains sufficient squares to record all data from $-h$ to $+h$ in one direction and from 0 to k in the other direction (or whatever indices the summation is to include).

Another sheet contains the four next tables to be filled in (Tables 2-5). Table 2 is for performing the operation of either adding $F_{hk} + F_{\bar{h}k}$ or subtracting $F_{hk} - F_{\bar{h}k}$ (or whatever the function may be). Strips are then selected to correspond to the numbers in a horizontal row of Table 2 and the usual summation is performed. The

* The original idea behind the arrangement of the present form was suggested by Miss Gabrielle Hamburger.

Table 1

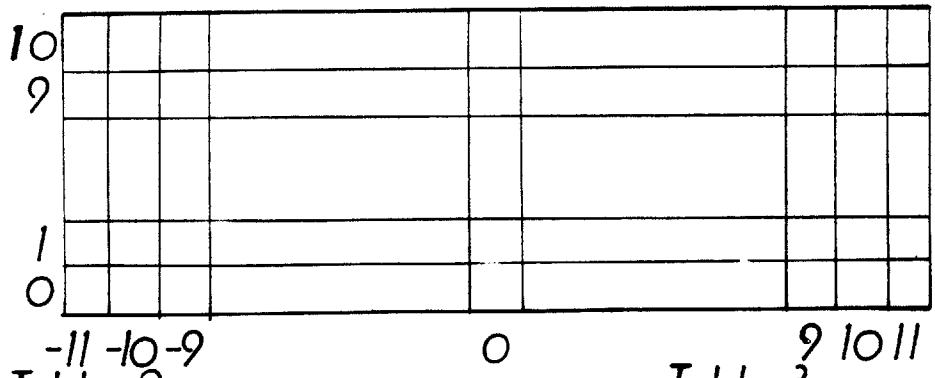

Table 2

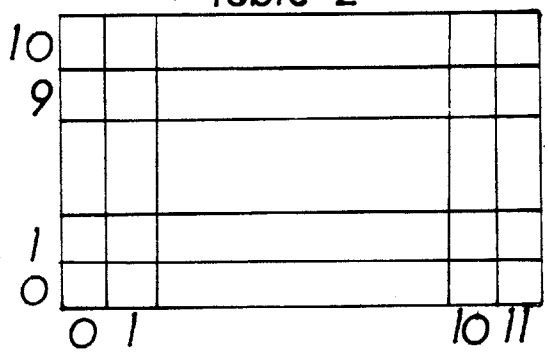

Table 3

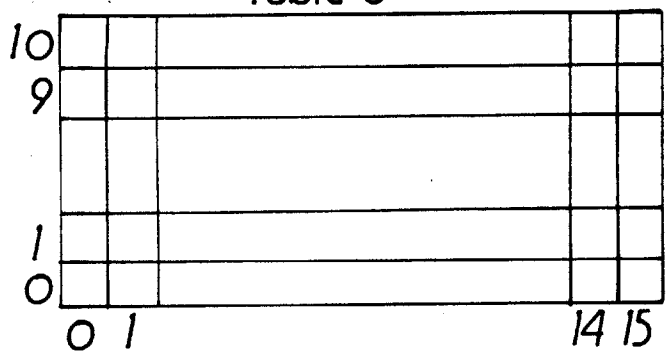

Table 4

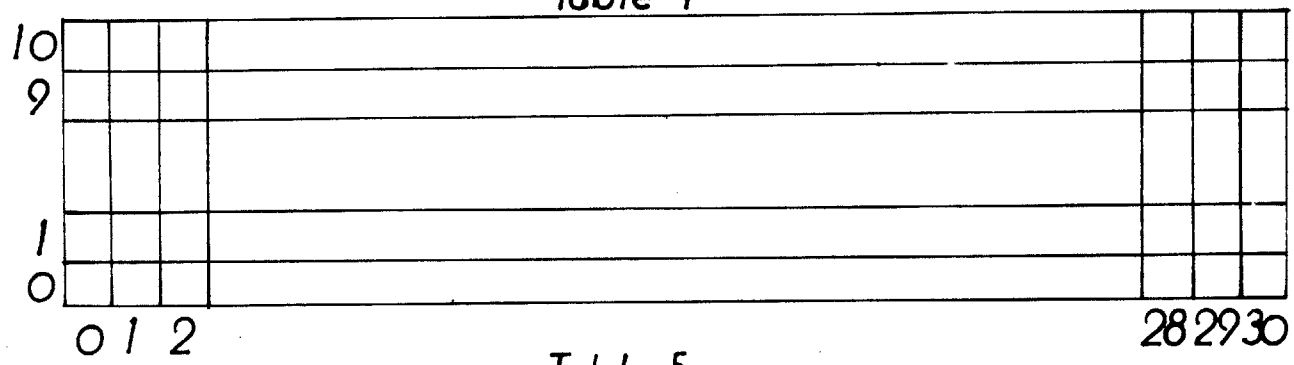

Table 5

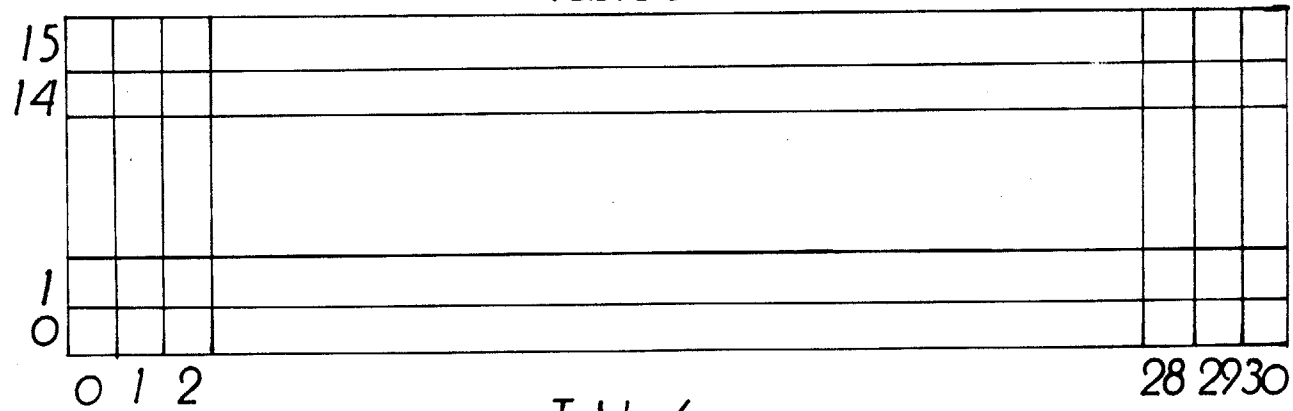

Table 6

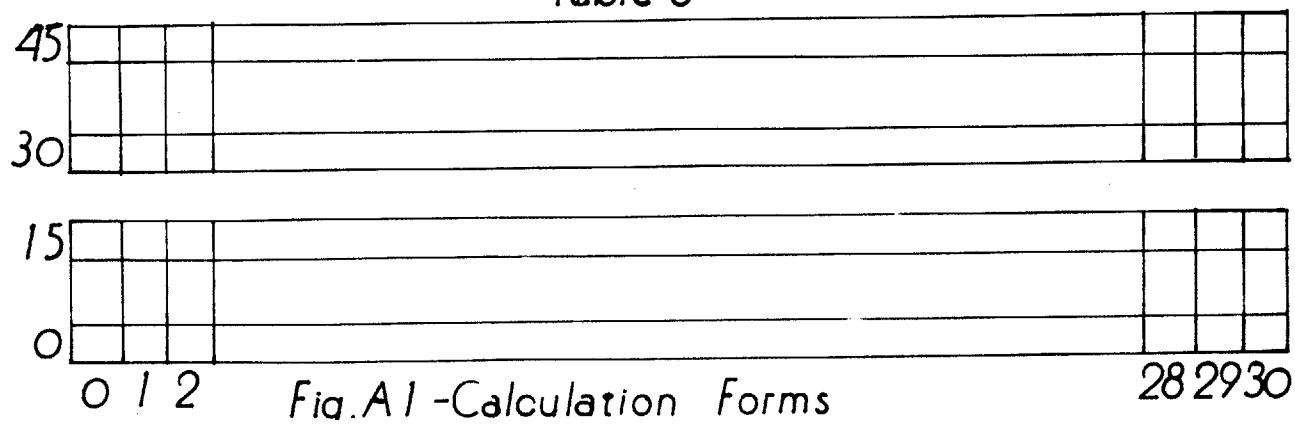

Fig. A1 -Calculation Forms

resulting answers are placed in the appropriate squares in Table 3, the odd terms being placed in the upper part of the box and the even terms in the lower part.

The two numbers in each box are then added up and the sum placed in the corresponding row and column in Table 4 for numbers from 0 to 15. The table is then extended from 15 to 30 by changing the sign of either the upper or lower term in each box (depending upon the particular case-- for cosine summations the sign of the upper term is changed and for sine summations the sign of the lower term is changed) and readding the numbers and placing the answer in the appropriate box from 15 to 30.

The numbers in the vertical columns are next used as the coefficients for the strips selected and each column is summed, the results being placed in the appropriate squares in Table 5.

One sheet will then contain all of the data for the summation of either the sin or cosine series. A second identical sheet will contain the data resulting from the summation of the function which was not summed on the first sheet.

The two Tables 5 are then placed side by side and the numbers from corresponding boxes are then combined according to the following procedure and the results

entered in Table 6. Strips are cut which contain slots in both ends and each strip contains the formula which pertains to that part of the cell to which it is applicable. One strip is used to sum the numbers from 0 to 15/60, one from 15/60 to 30/60, another from 30/60 to 45/60, and the fourth from 45/60 to 60/60. The designations T_1, T_2, T_3, and T_4 refer respectively to the lower left entry, the upper left entry, the lower right entry, and the upper right entry. The designations of the four strips follow:

#1 - n = 0 to n = 15, where n = y

$$T_1 + T_2 - T_3 - T_4$$

#2 - n = 15 to n = 30, where n = (30 - y)

$$T_1 - T_2 + T_3 - T_4$$

#3 - n = 30 to n = 45, where n = (30 + y)

$$T_1 - T_2 - T_3 + T_4$$

#4 - n = 45 to n = 60, where n = (60 - y)

$$T_1 + T_2 + T_3 + T_4$$

In the above manner the final resulting data for half of the unit cell is obtained.

In the following sections the formula which is applicable for performing the various parts of each synthesis which has been reported in the text will be presented.

In the case of the Harker syntheses only one synthesis was necessary, while in the case of some of the sections as many as four complete syntheses were required as may be seen from the formulas presented.

B. - Harker Synthesis P(xyO) (Resultant Data was used to prepare the Harker Implication I3(xyO)

For the Harker synthesis P (xyO) the Patterson function takes the following form:

$$P(xyO) = \sum_{h}\sum_{k}\left(\sum_{l}|F_{hkl}|^2\right)\cos 2\pi(hx+ky)$$

The above formula implies summing over l the $|F|^2$ values for all reflections having h and k indices the same but varying in l. These sums are then used as the coefficients in Table 1 of Fig. A1. It must be remembered that only $\frac{1}{2}$ of the $|F|^2$ values is used for reflections having $l = 0$, this being due to the difference in multiplicity of occurance between reflections of the type (hkO) and those of the general (hkl) type. The Tables 2 then take the form of $F^2_{hkl} + F^2_{hkl}$ and $F^2_{hkl} - F^2_{hkl}$ respectively. The remainder of the synthesis is then perfectly straight forward.

C. - Harker Implication I6(xy$\frac{1}{2}$)

The Patterson function for this particular case assumes the form:

$$P(xy\tfrac{1}{2}) = \sum_{h=-\infty}^{\infty}\sum_{k} \left(\sum_{l=-\infty}^{\infty} (-1)^{l} |F_{hkl}|^2 \right) \cos 2\pi(hx + ky)$$

The summation between the brackets means that it is necessary to sum the $|F|^2$ values for all reflections with the same h and k values and with l even, and subtract from this the sum of the $|F|^2$ values for all reflections with the same h and k values and l odd, i.e.

$$\sum_{l} |F_{hkl_{even}}|^2 - \sum_{l} |F_{hkl_{odd}}|^2$$

These values are then used as the coefficients entered in Table 1. The Tables 2 then take the form of $F^2_{hkl} + F^2_{\bar{h}kl}$ and $F^2_{hkl} - F^2_{\bar{h}kl}$ respectively.

D. - Electron density projection $\varrho(xy0)$

The formula applicable to this case is as follows:

$$\varrho(xy0) = \sum_{h=-\infty}^{\infty}\sum_{k} \left(\sum_{l=0} F_{hk0} \right) \cos 2\pi(hx + ky)$$

For this synthesis the F_{hk0} values are used just as they appear as the coefficients entered in Table 1. The sign (+ or -) assigned to each reflection is obtained from the theoretical intensity calculations and is dependent on the atomic parameters assigned to the various atoms. The Tables 2 then represent $F_{hk0} + F_{\bar{h}k0}$ and $F_{hk0} - F_{\bar{h}k0}$ respectively.

E. - One-dimensional Harker projections $P(x_1y_1z)$

The formulas applicable to the four one-dimensional Harker projections are as follows:

(1) $P(1/3,2/3,z) = \sum_{h}^{\infty}\sum_{k}\sum_{\ell} |F_{hk\underline{l}}|^2 \cos 2\pi (\frac{1}{3}h + \frac{2}{3}k + \underline{l}z)$

(2) $P(00z) = \sum_{h}^{\infty}\sum_{k}\sum_{\ell} |F_{hk\underline{l}}|^2 \cos 2\pi (\underline{l}z)$

(3) $P(.45,.45,z) = \sum_{h}^{\infty}\sum_{k}\sum_{\ell} |F_{hk\underline{l}}|^2 \cos 2\pi (.45h + .45k + \underline{l}z)$

(4) $P(.33,.23,z) = \sum_{h}^{\infty}\sum_{k}\sum_{\ell} |F_{hk\underline{l}}|^2 \cos 2\pi (.33h + .23k + \underline{l}z)$

A general discussion will serve to illustrate the procedure followed in all of the projections. For any ($hk\underline{l}$) reflection it becomes necessary to calculate the value of the term $\cos 2\pi(hx+ky+\underline{l}z)$ for a particular value of $\underline{z}$ and then to multiply this value by the $|F|^2$ value for the same reflection. The product is then multiplied by a factor of 12 for any ($hk\underline{l}$) reflection due to the multiplicity of combinations of ($hk\underline{l}$) for the space group $H6_3$. For any (hk0) reflection the product is multiplied by a factor of 6 and for any (h00) reflection the combinations are but two, and thus, the product for (h00) reflections is multiplied by a factor of 2. To simplify matters the actual multiplication factors employed are 6, 3, and 1 respectively.

The remaining step is merely to add up all of the values and the resultant sum gives the values of the function

at a particular value of z. The procedure is next repeated for another value of z and so on until a value of the function has been found for each assumed value of z.

The above is most easily accomplished by a perfectly straight forward longhand method of calculation.

F. - Electron density projection $\varrho(x_1 2x_1 z)$ [Projection on$(1\bar{2}10)$]

The formula applicable to this case is:

$$\varrho(x_1 2x_1 z) = \sum_{-\infty}^{\infty}\sum_{h}\sum_{l} A_{hO\underline{l}} \cos 2\pi(hx+\underline{l}z) + B_{hO\underline{l}} \sin 2\pi(hx+\underline{l}z)$$

Let $\cos 2\pi(hx+\underline{l}z) = A(x_1 2x_1 z)$

and $\sin 2\pi(hx+\underline{l}z) = B(x_1 2x_1 z)$

The values of $A_{hO\underline{l}}$ and $B_{hO\underline{l}}$ are in reality A_o and B_o as discussed in Chapter V and are computed for all of the $(hO\underline{l})$ reflections. The form illustrated in Fig. A2 is now followed where the following entries are made:

(1) $A_{hO\underline{l}} + A_{\bar{h}O\underline{l}} = CC_{hO\underline{l}}$

(2) $\sum_{-\infty}^{\infty}\sum_{h}\sum_{l} CC_{hO\underline{l}} \cos 2\pi hx \cos 2\pi \underline{l}z = CC_{(XZ)}$

In the above and in what follows the term (XZ) will be used to signify $(x_1 2x_1 z)$ in shorthand form.

On a second sheet (corresponding to the sine sheet for the Harker syntheses, the following entries are made:

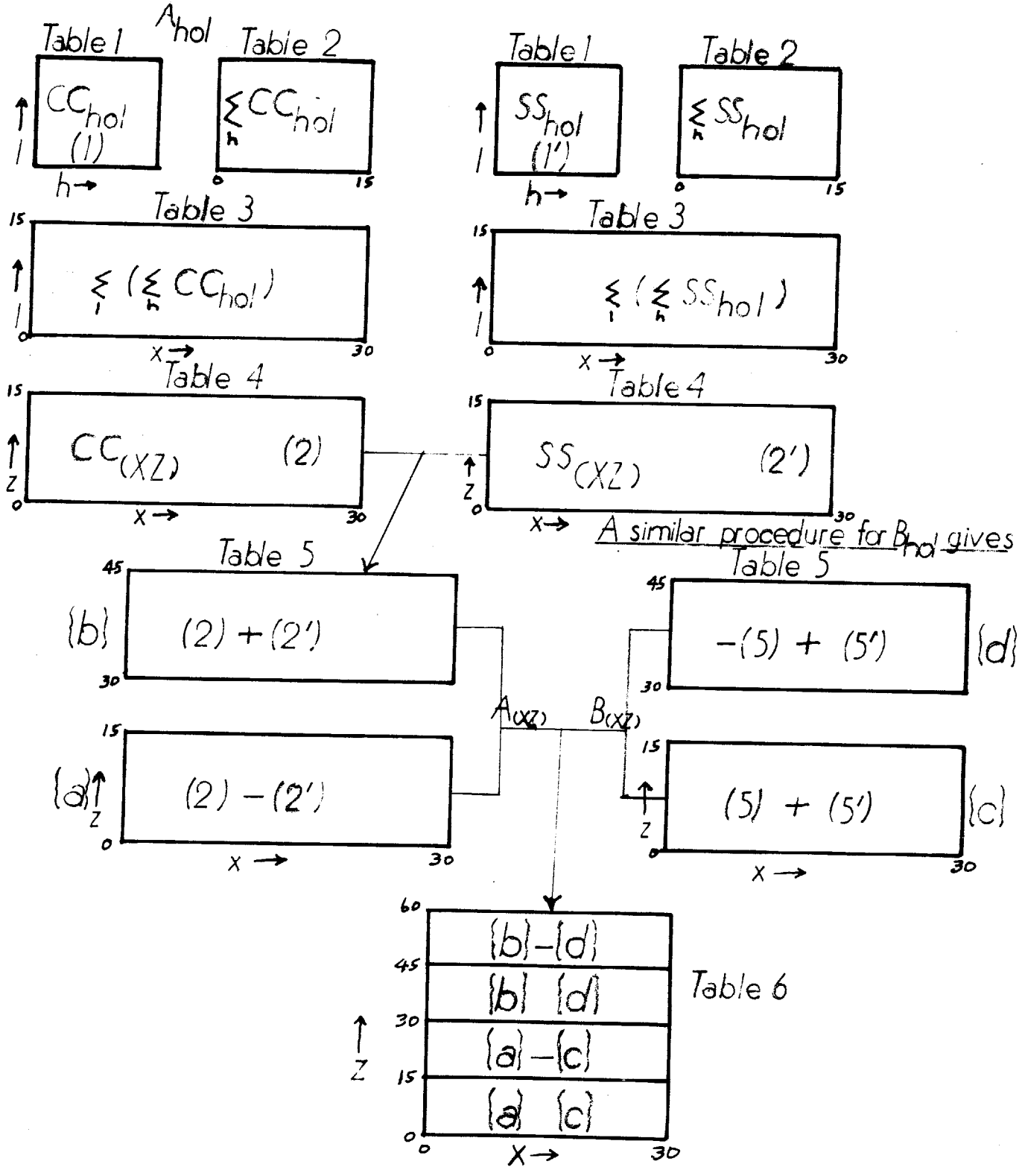

Fig. A 2 – Schematic Form of Computations for Non-Centrosymmetrical Sections and Electron Density Projections

(1') $A_{h0\underline{l}} - A_{\bar{h}0\underline{l}} = SS_{h0\underline{l}}$

(2') $\sum_{-\infty}^{\infty}\sum_{h\,l} SS_{h0\underline{l}} \sin 2\pi hx \sin 2\pi \underline{l}z = SS(XZ)$

(2) and (2') are next combined to give

$$\sum_{-\infty}^{\infty}\sum_{h\,l} A_{h0\underline{l}} \cos 2\pi(hx+\underline{l}z) = A(XZ) \ldots\ldots (3)$$

It must be noted that for (1) and (1') $|A_{h0\underline{l}}| = |A_{\bar{h}0\underline{l}}|$, so that $A_{h0\underline{l}} + A_{\bar{h}0\underline{l}}$ values are double the values for $A_{h0\underline{l}}$ alone when $\underline{l}$ is even and zero when $\underline{l}$ is odd, while for $A_{h0\underline{l}} - A_{\bar{h}0\underline{l}}$ the reverse is true. The values for reflections having either $\underline{h}$ or $\underline{l}$ equal to zero are merely $A_{h0\underline{l}}$ for (1) and zero for (1').

The entire procedure is now repeated for the $\underline{B}$ values where:

(4) $B_{h0\underline{l}} + B_{h0\bar{\underline{l}}} = SC_{h0\underline{l}}$

(5) $\sum_{-\infty}^{\infty}\sum_{h\,l} SC_{h0\underline{l}} \sin 2\pi hx \cos 2\pi \underline{l}z = SC(XZ)$

and

(4') $B_{h0\underline{l}} - B_{h0\bar{\underline{l}}} = CS_{h0\underline{l}}$

(5') $\sum_{-\infty}^{\infty}\sum_{h\,l} CS_{h0\underline{l}} \cos 2\pi hx \sin 2\pi \underline{l}z = CS(XZ)$

(5) and (5') are next combined to give

$$\sum_{-\infty}^{\infty}\sum_{h\,l} B_{h0\underline{l}} \sin 2\pi(hx+\underline{l}z) = B(XZ) \ldots\ldots (6)$$

The final summations (3) and (6) are next combined to give the final data for half of the unit cell according to the rules presented in Table 6 of Fig. A2. The entire above procedure is schematically illustrated in Fig. A2.

Thus, the electron density projection $\varrho(x_1 2x_1 z)$ is performed by employing the A_o and B_o values for the (h0$\underline{1}$) reflections and going through the summations as outlined above. The final data as obtained in Table 6 is then projected on to the plane of projection $(1\bar{2}10)$ as illustrated on page 89.

G. $\varrho(xy\frac{1}{4})$ Section

$$\varrho(xy\tfrac{1}{4}) = \sum_{h}\sum_{k}\sum_{l=-\infty}^{\infty} F_{hkl}\, e^{-2\pi i(hx+ky+\frac{l}{4})}$$

$$= \sum_{h}\sum_{k}\sum_{l=-\infty}^{\infty} A_{hkl} \cos 2\pi(hx+ky+\tfrac{l}{4})$$

$$+ \sum_{h}\sum_{k}\sum_{l=-\infty}^{\infty} B_{hkl} \sin 2\pi(hx+ky+\tfrac{l}{4})$$

$$\sum_{h}\sum_{k}\sum_{l=-\infty}^{\infty} A_{hkl} \cos 2\pi(hx+ky+\tfrac{l}{4}) = \sum_{h}\sum_{k}\sum_{l=-\infty}^{\infty} A_{hkl} \cos 2\pi\left[(hx+ky)+(\tfrac{l}{4})\right]$$

$$= \sum_{h}\sum_{k=-\infty}^{\infty} A_{hkl} \cos 2\pi(hx+ky) \cos 2\pi(\tfrac{l}{4})$$

$$- \sum_{h}\sum_{k=-\infty}^{\infty} A_{hkl} \sin 2\pi(hx+ky) \sin 2\pi(\tfrac{l}{4})$$

$$= \sum_{h}\sum_{k=-\infty}^{\infty} \cos 2\pi(hx+ky)\cdot A_{hkl} \sum_{l=-\infty}^{\infty} \cos 2\pi(\tfrac{l}{4})$$

$$- \sum_{h}\sum_{k=-\infty}^{\infty} \sin 2\pi(hx+ky)\cdot A_{hkl} \sum_{l=-\infty}^{\infty} \sin 2\pi(\tfrac{l}{4})$$

$$\sum_{h}\sum_{k}\sum_{l=-\infty}^{\infty} B_{hkl} \sin 2\pi(hx+ky+\tfrac{l}{4}) = \sum_{h}\sum_{k}\sum_{l=-\infty}^{\infty} B_{hkl} \sin 2\pi\left[(hx+ky)+(\tfrac{l}{4})\right]$$

$$= \sum_{h}\sum_{k=-\infty}^{\infty} B_{hkl} \sin 2\pi(hx+ky) \cos 2\pi(\tfrac{l}{4})$$

$$+ \sum_{h}\sum_{k=-\infty}^{\infty} B_{hkl} \cos 2\pi(hx+ky) \sin 2\pi(\tfrac{l}{4})$$

$$= \sum_{h}\sum_{k=-\infty}^{\infty} \sin 2\pi(hx+ky)\cdot B_{hkl} \sum_{l=-\infty}^{\infty} \cos 2\pi(\tfrac{l}{4})$$

$$+ \sum_{h}\sum_{k=-\infty}^{\infty} \cos 2\pi(hx+ky)\cdot B_{hkl} \sum_{l=-\infty}^{\infty} \sin 2\pi(\tfrac{l}{4})$$

$$\varrho(xy\tfrac{1}{4}) = A_{hkl} \sum_{l=-\infty}^{\infty} \cos 2\pi(\tfrac{l}{4}) \sum_{h}\sum_{k=-\infty}^{\infty} \cos 2\pi(hx+ky)$$

$$- A_{hkl} \sum_{l=-\infty}^{\infty} \sin 2\pi(\tfrac{l}{4}) \sum_{h}\sum_{k=-\infty}^{\infty} \sin 2\pi(hx+ky)$$

$$+ B_{hkl} \sum_{l=-\infty}^{\infty} \cos 2\pi(\tfrac{l}{4}) \sum_{h}\sum_{k=-\infty}^{\infty} \sin 2\pi(hx+ky)$$

$$+ B_{hkl} \sum_{l=-\infty}^{\infty} \sin 2\pi(\tfrac{l}{4}) \sum_{h}\sum_{k=-\infty}^{\infty} \cos 2\pi(hx+ky)$$

Each of the four terms in the final sum is treated as a separate synthesis. The first portion of each term, however, is subject to further considerations.

According to Lonsdale[32]:

For $l = 2n$: $\alpha(hk\underline{l}) = -\alpha(\overline{hk\underline{l}}) = -\alpha(hk\underline{\bar{l}})$

Therefore, $A_{hk\underline{l}} = A_{\overline{hk\underline{l}}} = A_{hk\underline{\bar{l}}}$

and $B_{hk\underline{l}} = -B_{\overline{hk\underline{l}}} = -B_{hk\underline{\bar{l}}}$

Thus:

$$1)\ \sum_{-\infty}^{\infty} A_{hk\underline{l}} \cos 2\pi\left(\frac{l}{4}\right) = \sum_{l}'^{\infty} \left(A_{hk\underline{l}} \cos 2\pi\left(\frac{l}{4}\right) + A_{hk\underline{l}} \cos 2\pi\left(\frac{l}{4}\right) + A_{hk0} \cos 2\pi\left(\frac{l}{4}\right)\right)$$

$$= \sum_{l}'^{\infty} \left(2\, A_{hk\underline{l}} + A_{hk0}\right) \cos 2\pi\left(\frac{l}{4}\right)$$

$$2)\ \sum_{-\infty}^{\infty} A_{hk\underline{l}} \sin 2\pi\left(\frac{l}{4}\right) = \sum_{l}'^{\infty} \left(A_{hk\underline{l}} \sin 2\pi\left(\frac{l}{4}\right) + A_{hk\underline{\bar{l}}} \sin 2\pi\left(\frac{\bar{l}}{4}\right) + A_{hk0} \sin 0\right)$$

$$= \sum_{l}'^{\infty} A_{hk\underline{l}} \sin 2\pi\left(\frac{l}{4}\right) - A_{hk\underline{l}} \sin 2\pi\left(\frac{l}{4}\right) = 0$$

$$3)\ \sum_{-\infty}^{\infty} B_{hk\underline{l}} \cos 2\pi\left(\frac{l}{4}\right) = \sum_{l}'^{\infty} \left(B_{hk\underline{l}} \cos 2\pi\left(\frac{l}{4}\right) + B_{hk\underline{\bar{l}}} \cos 2\pi\left(\frac{l}{4}\right) + B_{hk0} \cos 2\pi\left(\frac{l}{4}\right)\right)$$

$$= \sum_{l}'^{\infty} B_{hk\underline{l}} \cos 2\pi\left(\frac{l}{4}\right) - B_{hk\underline{l}} \cos 2\pi\left(\frac{l}{4}\right) = 0$$

$$4)\ \sum_{-\infty}^{\infty} B_{hk\underline{l}} \sin 2\pi\left(\frac{l}{4}\right) = \sum_{l}'^{\infty} \left(B_{hk\underline{l}} \sin 2\pi\left(\frac{l}{4}\right) + B_{hk\underline{\bar{l}}} \sin 2\pi\left(\frac{\bar{l}}{4}\right) + B_{hk0} \sin 2\pi\left(\frac{l}{4}\right)\right)$$

where $B_{hk\bar{1}} \sin 2\pi(\frac{\bar{\ell}}{4}) = - B_{hk\underline{1}} \cdot - \sin 2\pi(\frac{\ell}{4})$

$$= \sum_{\ell}' (2\ B_{hk\underline{1}} + B_{hk0}) \sin 2\pi(\tfrac{\ell}{4})$$

For $l = 2n+1$: $\alpha(hk\underline{1}) = \pi - \alpha(hk\bar{1})$

Therefore, $A_{hk\underline{1}} = - A_{hk\bar{1}}$

and $B_{hk\underline{1}} = B_{hk\bar{1}}$

Thus:

1) $\sum_{-\infty}^{\infty} A_{hk\underline{1}} \cos 2\pi(\frac{\ell}{4}) = \sum_{\ell}' A_{hk\underline{1}} \cos 2\pi(\frac{\ell}{4}) + A_{hk\bar{1}} \cos 2\pi(\frac{\bar{\ell}}{4}) = 0$

2) $\sum_{-\infty}^{\infty} A_{hk\underline{1}} \sin 2\pi(\frac{\ell}{4}) = \sum_{\ell}' (A_{hk\underline{1}} \sin 2\pi(\frac{\ell}{4}) + A_{hk\bar{1}} \sin 2\pi(\frac{\bar{\ell}}{4})$

$$+ A_{hk0} \sin 2\pi(\tfrac{\ell}{4}))$$

$$= \sum_{\ell}' (2\ A_{hk\underline{1}} + A_{hk0}) \sin 2\pi(\tfrac{\ell}{4})$$

3) $\sum_{-\infty}^{\infty} B_{hk\underline{1}} \cos 2\pi(\frac{\ell}{4}) = \sum_{\ell}' (B_{hk\underline{1}} \cos 2\pi(\frac{\ell}{4}) + B_{hk\bar{1}} \cos 2\pi(\frac{\bar{\ell}}{4})$

$$+ B_{hk0} \cos 2\pi(\tfrac{\ell}{4}))$$

$$= \sum_{\ell}' (2\ B_{hk\underline{1}} + B_{hk0}) \cos 2\pi(\tfrac{\ell}{4})$$

4) $\sum_{-\infty}^{\infty} B_{hk\underline{1}} \sin 2\pi(\frac{\ell}{4}) = \sum_{\ell}' (B_{hk\underline{1}} \sin 2\pi(\frac{\ell}{4}) + B_{hk\bar{1}} \sin 2\pi(\frac{\bar{\ell}}{4})$

$$+ B_{hk0} \sin 2\pi(\tfrac{\ell}{4}))$$

where $B_{hk\bar{1}} \sin 2\pi(\frac{\bar{\ell}}{4}) = B_{hk1} \cdot - \sin 2\pi(\frac{\ell}{4})$

$$= 0$$

It may be seen that for (hk$\underline{l}$) reflections where $\underline{l}$ is even the second and third terms always equal zero and drop out. For cases where $\underline{l}$ is odd, the first and fourth terms equal zero and always drop out. Hence, in the general case it is only necessary to compute the synthesis for $A_{hk\underline{l}} \sum_{l=-\infty}^{\infty} \cos 2\pi(\frac{l}{4}) \sum_{h}\sum_{k=-\infty}^{\infty} \cos 2\pi(hx+ky)$ and $B_{hk\underline{l}} \sum_{l=-\infty}^{\infty} \sin 2\pi(\frac{l}{4}) \sum_{h}\sum_{k=-\infty}^{\infty} \cos 2\pi(hx+ky)$ for the reflections having $\underline{l}$ even, and $-A_{hk\underline{l}} \sum_{l=-\infty}^{\infty} \sin 2\pi(\frac{l}{4}) \sum_{h}\sum_{k=-\infty}^{\infty} \sin 2\pi(hx+ky)$ and $B_{hk\underline{l}} \sum_{l=-\infty}^{\infty} \cos 2\pi(\frac{l}{4}) \sum_{h}\sum_{k=-\infty}^{\infty} \sin 2\pi(hx+ky)$ for reflections having $\underline{l}$ odd.

The value of $\cos 2\pi(\frac{l}{4}) = 0$ for $\underline{l}$ odd, $+1$ for $\underline{l}$ even and not divisible by 4, and -1 for $\underline{l}$ even and divisible by 4. The value of $\sin 2\pi(\frac{l}{4}) = 0$ for $\underline{l}$ even, $+1$ for $\underline{l}$ odd and $\underline{l} = 1,5,9$, and -1 for $\underline{l}$ odd and equal to 3,7,10.

The values of A_o and B_o as listed in Table XI do not take into account the multiplicity of occurance of the reflection to which it is assigned. Hence, the values of the A_o and B_o terms for (hOO) reflections are divided by a factor of 2, those for (hkO) reflections are maintained as they appear, and those for general (hk$\underline{l}$) reflections are multiplied by a factor of 2. These are the A_o and B_o values which are now used in all of the section syntheses.

The correct values of A_o and B_o are next multiplied by the correct trigonometric function and are summed for (hk$\underline{l}$) reflections having $\underline{h}$ and $\underline{k}$ constant and $\underline{l}$ varying for the even values of $\underline{l}$ only or the odd values of $\underline{l}$ only as the case may be. These values are then entered as the entries in Table 1. Two complete syntheses (in the usual sense of meaning) are then computed as illustrated in Fig. A2, one for the A_o values and the other for the B_o values, and the final results are obtained by adding the results of the final tables (Table 6) containing the results from the $\underline{A}$ summation and that from the $\underline{B}$ summation. Particular attention must be paid to the fact that the entire second $\underline{A}$ summation is negative and must be treated accordingly in the summations.

H. - ϱ(xOz) Section

The formula applicable to this section is:

$$\varrho(xOz) = \sum_{-\infty}^{\infty}\sum_{h}\sum_{k}\sum_{l} F_{hk\underline{l}}\, e^{-2\pi i(hx+\underline{l}z)}$$

$$= \sum_{-\infty}^{\infty}\sum_{h}\sum_{l} e^{-2\pi i(hx+\underline{l}z)} \sum_{-\infty}^{\infty}\sum_{k} F_{hk\underline{l}}$$

$$= \sum_{-\infty}^{\infty}\sum_{h}\sum_{l} e^{-2\pi i(hx+\underline{l}z)} \left(\sum_{-\infty}^{\infty}\sum_{k} A_{hk\underline{l}} + \sum_{-\infty}^{\infty}\sum_{k} B_{hk\underline{l}} \right)$$

$$\varrho(xOz) = \sum_{-\infty}^{\infty}\sum_{h}\sum_{l} A_{hk} \cos 2\pi(hx+ky) + \sum_{-\infty}^{\infty}\sum_{h}\sum_{l} B_{hk} \sin 2\pi(hx+ky)$$

This synthesis is performed in a manner identical with that just discussed, only that for the two Tables 1 the terms

are made up of the values of A_o and B_o for reflections having a constant h and l value and only k varying, according to the rules just presented. These sums are then used as the entries in Table 1 and the remainder of the synthesis is as illustrated in Fig. A2.

I. - $\varrho(xyO)$ Section

The formula applicable to this case is as follows:

$$\varrho(xyO) = \sum_{-\infty}^{\infty}\sum_{h}\sum_{k}\sum_{l} F_{hkl}\, e^{-2\pi i(hx+ky)}$$

$$= \sum_{-\infty}^{\infty}\sum_{h}\sum_{k} e^{-2\pi i(hx+ky)} \sum_{-\infty}^{\infty}\sum_{l} F_{hkl}$$

$$= \sum_{-\infty}^{\infty}\sum_{h}\sum_{k} e^{-2\pi i(hx+ky)} \left(\sum_{-\infty}^{\infty}\sum_{l} A_{hkl} + \sum_{-\infty}^{\infty}\sum_{l} B_{hkl}\right)$$

$$\varrho(xyO) = \sum_{-\infty}^{\infty}\sum_{h}\sum_{k} A_{hk} \cos 2\pi(hx+ky) + \sum_{-\infty}^{\infty}\sum_{h}\sum_{k} B_{hk} \sin 2\pi(hx+ky)$$

The procedure followed is identical with that performed for the section $\varrho(xOz)$ except that the data put into Table 1 consists of the correct values of A_o and B_o for reflections which have constant h and k values and l varies. The values of $\sum_{-\infty}^{\infty}\sum_{l} A_{hkl} \cos 2\pi(hx+ky)$ apply only to A_o values with l even, while the $\sum_{-\infty}^{\infty}\sum_{l} B_{hkl} \sin 2\pi(hx+ky)$ values apply only to the B_o values with l odd.

J. - $\varrho(x, 2/3, z)$ Section

By a proof identical with that just presented for the case of the $\varrho(xy\frac{1}{4})$ section, it is possible to arrive directly at the formula applicable to this section. The formula in its final form is:

$$\begin{aligned}\varrho(x,2/3,z) = {} & A_{hk\underline{l}} \sum_{K=-\infty}^{\infty} \cos 2\pi(2k/3) \sum_{h}\sum_{\underline{l}=-\infty}^{\infty} \cos 2\pi(hx+\underline{l}z) \\ & -A_{hk\underline{l}} \sum_{K=-\infty}^{\infty} \sin 2\pi(2k/3) \sum_{h}\sum_{K=-\infty}^{\infty} \sin 2\pi(hx+\underline{l}z) \\ & + B_{hk\underline{l}} \sum_{K=-\infty}^{\infty} \cos 2\pi(2k/3) \sum_{h}\sum_{\underline{l}=-\infty}^{\infty} \sin 2\pi(hx+\underline{l}z) \\ & + B_{hk\underline{l}} \sum_{K=-\infty}^{\infty} \sin 2\pi(2k/3) \sum_{h}\sum_{\underline{l}=-\infty}^{\infty} \cos 2\pi(hx+\underline{l}z)\end{aligned}$$

The procedure followed for the $\varrho(x,2/3,z)$ section is identical with that followed for the $\varrho(xy\frac{1}{4})$ section except that the values for A_o and B_o times the correct trigonometric function are summed for reflections with constant $\underline{h}$ and $\underline{l}$ values and $\underline{k}$ varying. These values are then entered in Table 1.

The value of $\cos 2\pi(2k/3) = +1$, where $\underline{k}$ is divisible by 3, and -.5 for all other values of $\underline{k}$. The values of $\sin 2\pi(2k/3) = 0$ for all values of $\underline{k}$ divisible by 3, $+.866$ for values of $\underline{k} = 2,5,8,11$, and -.866 for values of $\underline{k} = 1,4,7,10$.

BIBLIOGRAPHY

1. Bragg, W.L. - ATOMIC STRUCTURE OF MINERALS, Cornell University Press, 272 (1937).

2. Schiebold, E. - Neues Jahrb. Min. etc., Bl. Bd., 64A, 312-313 (1931).

3. Ford, W.E. - DANA'S TEXTBOOK OF MINERALOGY, 4th Edition, John Wiley and Sons, 585 (1932).

4. Baumhauer, H. - Zeit. Krist., 6, 209-216 (1882).

5. Baumhauer, H. - ibid., 18, 614 (1891).

6. Duboin, A. - Compt. Rend., 115, 56-57 (1892).

7. Duboin, A. - Bull. Soc. Franc. Mineral., 15, 191-194 (1892).

8. Baumhauer, H. - DIE RESULTATE DER ATZMETHODE IN DER KRISTALLOGRAPHICEN FORSCHUNG, Wilhelm Englemann, Leipzig (1894).

9. Bowen, N.L. and Ellestad, R.B. - Amer. Mineral., 21, 363-368 (1936).

10. Morozewicz, J. - Anzeiger der Akad. d. Wiss. in Krakau, 8, 958 (1897).

11. Bowen, N.L. - Trav. du Serv. Geol. de Pologne, 2, 314, (1929).

12. Bannister, F.A. and Hey, M.H. - Mineral. Mag., 22, 569-608 (1931).

13. Bowen, N.L. and Grieg, J.W. - Amer. J. Sci., 10, 204-212 (1925).

14. Gottfried, C. - Zeit. Krist, 65, 100-109 (1926).

15. Gossner, B. - Central. Mineral., Geol., Paleont., A-1927, 150-158 (1927).

16. Jaeger, F.M., Westenbrink, H.G.K., and Van Melle, F.A. - Proc. Sect. Sci. Akad. Wissen. Amsterdam, 30, 266 (1927).

17. Jaeger, F.M. - Bull. Soc. Franc. Mineral., 53, 183-209 (1930).

18. Schiebold, E. - Naturwiss., 18, 705-706 (1930).

19. Eitel, W., Herlinger, E., and Tromel, G. - Veroffent. Kaiser-Wilhelm Inst. Silicat. Forsch., 3, 103-131 (1930).

20. Nowacki, W. - Naturwiss, 30, 471-472 (1942).

21. Belov, N.V. - Vernadsky Jub. Vol. Acad. Sci. U.S.S.R., 1, 581-584 (1936).

22. Winchell, A.N. - Amer. Mineral., 26, 536-540 (1941).

23. Buerger, M.J. - X-RAY CRYSTALLOGRAPHY, John Wiley and Sons, (1942).

24. Buerger, M.J. - Proc. Nat. Acad. Sci., 26, 637-642, (1940).

25. Buerger, M.J. and Klein, G.E. - J. App. Phys., 16, 408-418, (1945).

26. Dawton, R.H.V.M. - Proc. Phys. Soc., 50, 919-925 (1938).

27. Patterson, A.L. - Phys. Rev., 46, 372-376 (1934).

28. Patterson, A.L. - Zeit. Krist., A 90, 517-542 (1935).

29. Harker, D. - J. Chem. Phys., 4, 381-390 (1936).

30. Buerger, M.J. - J. App. Phys., 17, 579-595 (1946).

31. Patterson, A.L. and Tunell, G. - Amer. Mineral., 27, 655-679 (1942).

32. Lonsdale, K. - STRUCTURE FACTOR TABLES, G. Bell and Sons Ltd., 112-113 (1936).

33. Buerger, M.J. - NUMERICAL STRUCTURE FACTOR TABLES, Geol. Soc. of Amer., special paper no. 33 (1941).

34. Buerger, M.J. and Klein, G.E. - J. App. Phys., 17, 285-306 (1946).

35. Bragg, W.L. - Nature, 138, 362-363 (1936).

36. Bragg, W.L. and Lipson, H. - Zeit. Krist., 95, 323-337 (1936).

37. Booth, A.D. - Phil. Mag., 36, 609 (1945).

38. Barth, T. - Amer. J. Sci., 24, 97 (1932).